KfK 5272
Januar 1994

Liquid Metal Flows in Manifolds and Expansions of Insulating Rectangular Ducts in the Plane Perpendicular to a Strong Magnetic Field

S. Molokov
Institut für Angewandte Thermo- und Fluiddynamik
Projekt Kernfusion

Kernforschungszentrum Karlsruhe

Kernforschungszentrum Karlsruhe
Institut für Angewandte Thermo- und Fluiddynamik
Projekt Kernfusion

KfK 5272

Liquid Metal Flows in Manifolds and Expansions of Insulating Rectangular Ducts in the Plane Perpendicular to a Strong Magnetic Field

S. Molokov

Kernforschungszentrum Karlsruhe GmbH, Karlsruhe

Kernforschungszentrum Karlsruhe GmbH
Postfach 3640, 76021 Karlsruhe

ISSN 0303-4003

Liquid Metal Flows in Manifolds and Expansions of Insulating Rectangular Ducts in the Plane Perpendicular to a Strong Magnetic Field

Abstract

Liquid metal flows in insulating rectangular ducts in strong magnetic fields are considered with reference to poloidal concepts of self-cooled blankets. Although major part of the flow in poloidal blanket concepts is close to being fully developed, manifolds, expansions, contractions, elbows, etc., which are necessary elements in blanket designs, cause three-dimensional effects. The present investigation demonstrates the flow pattern in basic insulating 3-D geometries for the actual and for more advanced liquid-metal blanket concepts and discusses the ways to avoid pressure losses caused by flow redistribution. Flows in several geometries, such as symmetric and non-symmetric 180° turns with and without manifolds, sharp elbows, sharp and linear expansions with and without manifolds, T-junction, etc., have been calculated. They demonstrate high reliability of poloidal concepts of liquid-metal blankets, since they guarantee uniform conditions for heat transfer. If changes of the duct cross-section occur in the plane perpendicular to the magnetic field (ideally a coolant should flow always in the radial-poloidal plane) the disturbances are local and the slug velocity profile is reached roughly at the distance equivalent to one duct width from the manifolds, expansions, etc. The effects of inertia in these flows are unimportant for the determination of the pressure drop and mean velocity profiles in the core of the flow but may favour heat transfer characteristics via instabilities and strongly anisotropic turbulence.

Flüssigmetallströmungen in isolierten Rechteckkanälen in Sammlern und Expansionen in einer Ebene senkrecht zu einem äußeren starken Magnetfeld

Zusammenfassung

Im Hinblick auf Anwendungen für selbstgekühlte Flüssigmetall-Blankets werden Flüssigmetallströmungen in isolierten rechteckförmigen Kanälen unter Einwirkung äußerer starker Magnetfelder untersucht. Obwohl in poloidalen Blanketkonzepten die Strömung nahezu voll ausgebildet ist, werden in Verzweigungen, Erweiterungen, Verengungen, Krümmern etc. dreidimensionale Effekte erzeugt. In dieser Arbeit werden Strömungsstrukturen in isolierten, dreidimensionalen Basisgeometrien für aktuelle und fortgeschrittenere Flüssigmetall-Blankets diskutiert und Wege aufgezeigt, wie Druckverluste hervorgerufen durch Strömungsumverteilung vermieden werden können. Strömungen in unterschiedlichen Geometrien, wie z.B. in symmetrischen und asymmetrischen Umlenkungen mit und ohne Verzweigung, in scharfkantigen Krümmern, in linearen Expansionen mit und ohne Verzweigung, in T-Stücken, etc. werden berechnet. Sie erhöhen die Zuverlässigkeit von poloidalen Flüssigmetallkonzepten, da sie homogene Wärmeübertragungsbedingungen garantieren. Falls Querschnittsveränderungen in einer Ebene senkrecht zum Magnetfeld auftreten (unter idealen Bedingungen sollte das Kühlmittel in der poloidal- radialen Ebene fließen) sind Störungen lokal, und das kolbenförmige Geschwindigkeitsprofil wird etwa nach einer Lauflänge erreicht, die mit der Breite der Expansion oder des Verteilers vergleichbar ist. Trägheitseffekte in diesen Strömungen sind unwichtig für die Bestimmung des Druckverlusts und der mittleren Strömungsgeschwindigkeit. Durch das Auftreten von Instabilitäten und stark anisotroper Turbulenz können sie jedoch den Wärmeübergang günstig beeinflussen.

Contents

1.	**Introduction**	**9**
2.	**Formulation**	**11**
3.	**General discussion**	**13**
4.	**Flow analysis at large Hartmann numbers**	**18**
	4. 1 Core region	19
	4. 2 Side layer at z=-L	20
5.	**Flows in basic blanket elements**	**23**
	Symmetric 180°-turn	24
	Non-symmetric 180°-turn	25
	Non-symmetric 180°-turn with manifold	26
	Manifold distributing liquid metal from one straight duct to several	28
	Sharp expansion	30
	Sharp expansion with manifold	31
	Linear expansion	32
	T-junction	34
	Sharp elbow	40
6.	**Inertia effects**	**42**
7.	**Conclusions**	**45**
8.	**References**	**47**

1. Introduction

Blanket-relevant research in liquid-metal magnetohydrodynamics has been recently shifted towards the flows in ducts with insulating walls. Although it was realised even at the early stage of blanket development that insulation of duct walls solves many of the problems of self-cooled liquid-metal blankets, it was unclear if an effective insulation can really be achieved. The progress in material research of insulating coatings which would cover electrically conducting walls and withstand high irradiation and mechanical stress made it possible to consider self-cooled blankets with insulating walls as a real option. As a result two new blanket concepts have been presented almost simultaneously by Sze *et al.* (1992) and Malang *et al.* (1993). Both of them are poloidal concepts which involve very simple (from magnetohydrodynamic point of view) flows in rectangular ducts in a transverse magnetic field as the main elements of the cooling system. A schematic diagram of the dual-coolant concept of blanket (Malang *et al.* 1993) is shown in Fig. 1.

One of the advantages of flows in straight insulating ducts with respect to those in ducts with conducting walls is that in the former the pressure drop per unit length grows only linearly with B_0, the induction of the uniform transverse magnetic field, while in the latter it grows as B_0^2. Since in tokamaks B_0~5-10T, the difference is very high. The other advantage is a slug velocity profile in a straight insulating duct that implies uniform conditions for heat removal due to internal heating and for cooling the first wall.

Although the major part of the flow in poloidal blanket concepts is close to being fully developed, elements such as manifolds, expansions, contractions, elbows, etc. cause three-dimensional effects. If changes of duct cross-section occur in the direction of the strong magnetic field, or if magnetic field induction varies in the flow direction, the additional pressure drop due to three-dimensional effects in inertialess flow increases as $B_0^{\frac{3}{2}}$ and the fluid velocity in the core close to the 3-D elements is strongly reduced (Walker, Ludford & Hunt, 1972, Lavrentiev *et al.*, 1990). In contrast, changes of the cross-section in the plane perpendicular to the magnetic field do not cause considerable three-dimensional effects. The present investigation concentrates on the latter flows in order to demonstrate the flow structure in basic insulating 3-D geometries and to show how to avoid pressure losses caused by flow redistribution in self-cooled liquid-metal blankets.

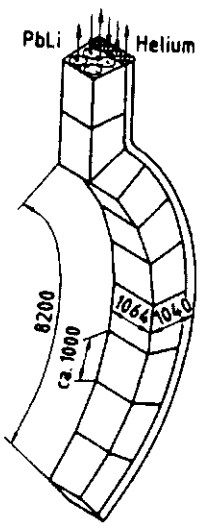

Fig. 1a

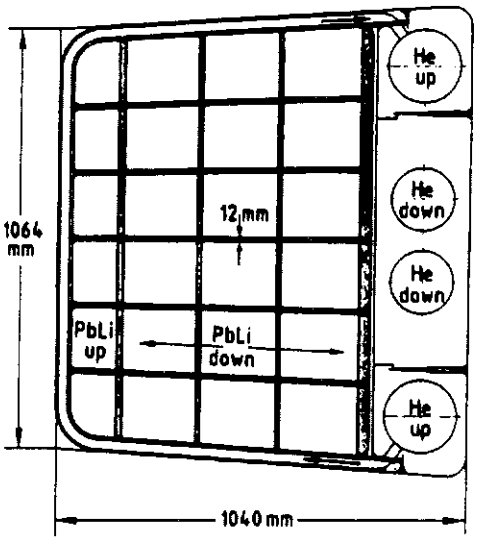

Fig. 1b

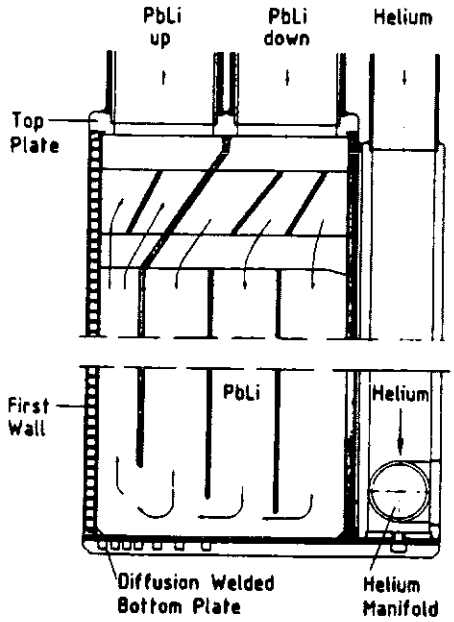

Fig. 1c

Fig. 1. Dual coolant liquid metal breeder blanket (from Malang *et al.* 1993). **a)** outboard blanket segment; **b)** cross-section of an outboard blanket segment; **c)** upper and lower end of the blanket segment.

2. Formulation

Consider the steady flow of a viscous, electrically conducting, incompressible fluid in a rectangular duct (Fig. 2) or in the system of rectangular ducts (manifold). The duct consists of a straight part, which is in general connected to a variable-area part. The axis of the variable-area duct may be curvilinear. All walls of the ducts are electrically insulating. The x-coordinate points in the main-flow direction in the straight part. One pair of the duct walls, called the side walls, is parallel to the strong uniform magnetic field $\underline{B} = B_0\hat{y}$. The other pair of walls (top and bottom walls, which are also called the Hartmann walls) is perpendicular to the field in the straight part, or in general is inclined to the field.

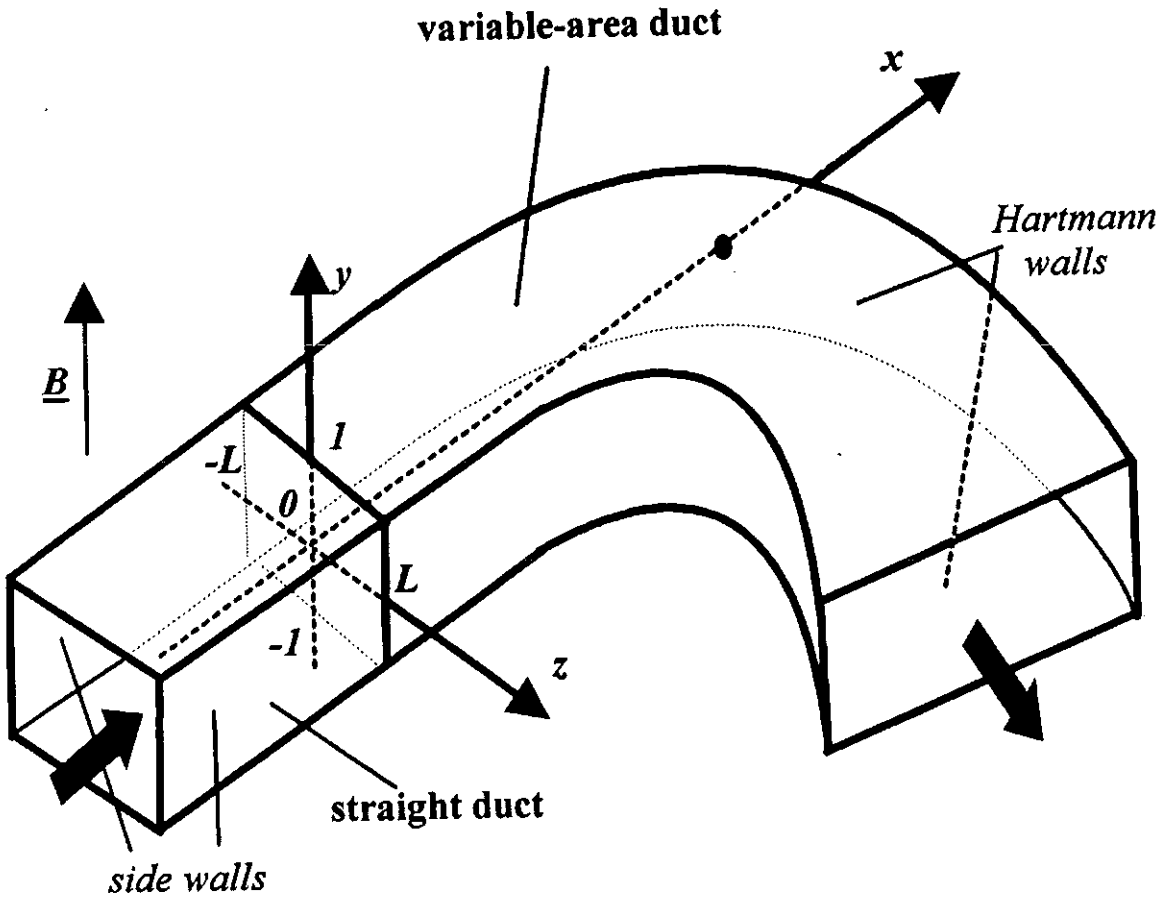

Fig. 2 Flow in the variable-area duct

The dimensionless inductionless equations governing the flow are

$$M^{-2}\nabla^2 \underline{v} + \underline{j} \times \hat{y} = \nabla p + N^{-1}(\underline{v} \cdot \nabla)\underline{v}, \tag{1a}$$

$$\underline{j} = -\nabla\phi + \underline{v} \times \hat{y}, \tag{1b}$$

$$\nabla \cdot \underline{v} = 0, \tag{1c}$$

$$\nabla \cdot \underline{j} = 0, \tag{1d}$$

where $M = B_0 a\sqrt{\sigma/\rho\nu}$ is the Hartmann number, $N = \sigma a B_0^2/\rho v_0$ is the interaction parameter, a is half the distance between the Hartmann walls in the straight part, σ, ρ, ν are electrical conductivity, density and kinematic viscosity of the fluid, respectively. The fluid velocity $\underline{v} = u\hat{x} + v\hat{y} + w\hat{z}$, the electric current density $\underline{j}$, the electric potential ϕ and the pressure p are normalised by v_o (average fluid velocity in the straight part), $v_o B_o \sigma$, $v_0 B_0 a$ and $\sigma v_0 B_0^2 a$, respectively.

The boundary conditions at each wall are the non-slip condition

$$\underline{v} = 0 \tag{1e}$$

and the electrical condition for an insulating wall

$$\underline{j} \cdot \hat{n} = 0, \tag{1f}$$

where $\hat{n}$ is the normal unit vector to the wall. The condition of constant mass flux

$$\int_{-1}^{1} dy \int_{-L}^{L} u dz = 4L \qquad \text{as } x \to -\infty \tag{1g}$$

normalises the solution to the problem (1a-f).

3. General discussion

Straight poloidal constant-area rectangular ducts with one pair of walls parallel to the strong toroidal magnetic field are main elements of a cooling system in poloidal concepts of self-cooled liquid-metal blankets. For flows in such ducts with insulating walls the exact solution to the problem (1) has been obtained by Shercliff (1953), who presents the expression for the fluid velocity, which is valid for arbitrary values of parameters M and L, in the form

$$u = 2k\sum_{n=1}^{\infty}\frac{(-1)^n}{\beta_n^3}\left\{1+\frac{\cosh m_1 y \sinh m_2 - \cosh m_2 y \sinh m_1}{\sinh \gamma_n}\right\}\cos\beta_n z, \qquad (2)$$

where $\beta_n = (n-\frac{1}{2})\pi / L$, $m_{1,2} = \frac{1}{2}\{-M \pm \gamma_n\}$, $\gamma_n = \sqrt{M^2+4\beta_n^2}$ and the absolute value of the constant pressure gradient $k = -dp/dx$ is

$$k = M^{-2}L\left[\sum_{n=1}^{\infty}\beta_n^{-4}\left\{1+\frac{\gamma_n(\cosh M - \cosh\gamma_n)}{\beta_n^2 \sinh\gamma_n}\right\}\right]^{-1}. \qquad (3)$$

The velocity profiles and the pressure gradient for the square duct and for different values of the Hartmann number are shown in Figs. 3 and 4. Due to fully developed, unidirectional nature of the flow inertia terms vanish identically and parameter the N does not enter the steady solution (2), (3).

The parameter M relevant to lithium-lead blanket conditions (Malang *et al.*, 1993) is very high (8000-18000), while N varies from moderate to high values (160-2500). For lithium blankets the values of N are at least one order higher. In any case $M>>1$ and $N>>1$, so that under blanket relevant conditions the flow exhibits certain asymptotic properties.

Figure 3 demonstrates that for M higher than 50 the flow region consists of the inviscid core, which occupies the bulk of the fluid, where velocity is constant (slug velocity profile), and thin boundary layers at the duct walls. The thickness of the layers at the Hartmann walls is $O(M^{-1})$, while the thickness of the side layers at the side walls is $O(M^{-\frac{1}{2}})$ (Fig. 3g). Viscous effects are confined to the boundary layers. The electric currents are induced in the core in the z-direction and return back in the layers (Fig. 3f). The asymptotic analysis of the flow for $M>>1$ was performed by Shercliff (1953), who derived asymptotic expressions for the fluid velocity in the core, the Hartmann- and the side- layers (see also Roberts 1967, Temperley 1976, Moreau 1990). The experiments of Branover & Gelfgat (1968), performed for M=174, Re=25300 (N=1.19) and Re=40200 (N=0.75) confirmed Shercliff's results and the asymptotic flow structure even for relatively low values of M and N. Here $\mathrm{Re} = av_0 / \nu$ is the Reynolds number.

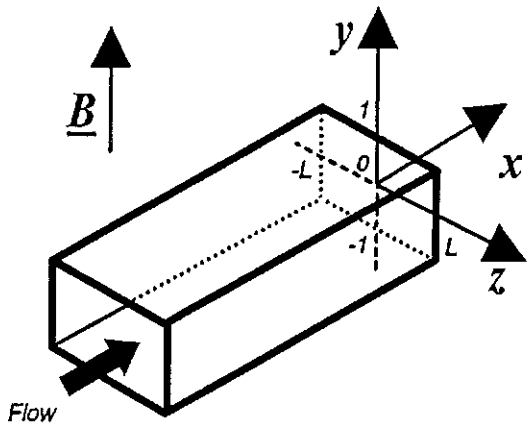

Fig. 3a

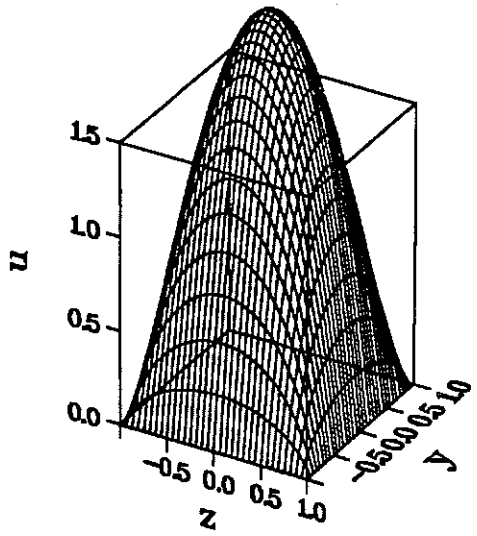

Fig. 3b M=0

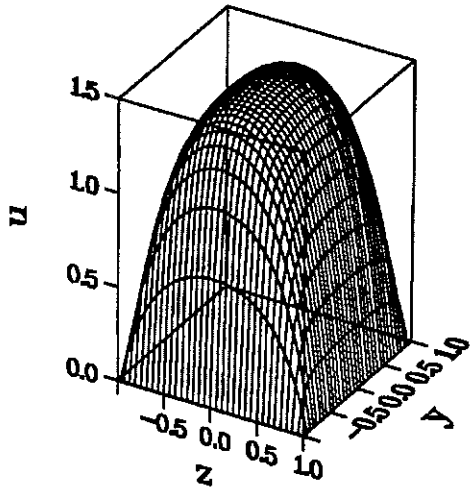

Fig. 3c M=10

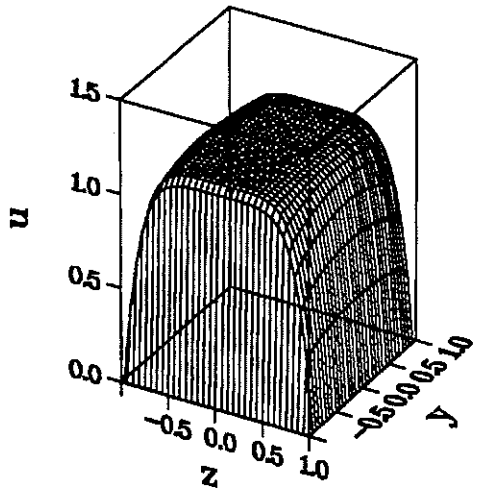

Fig. 3d M=50

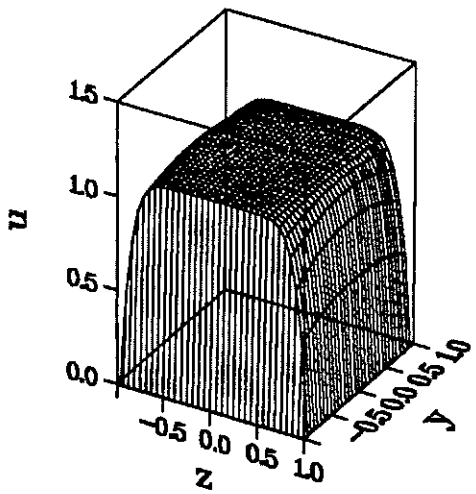

Fig. 3e M=100

Fig. 3 Flow in a straight rectangular duct with insulating walls (Shercliff's exact solution). **a)** flow scheme; **b-e)** fluid velocity for L=1 and for different values of the Hartmann number; **f)** lines of electric current for M=100, L=1; **g)** flow subregions at high Hartmann number.

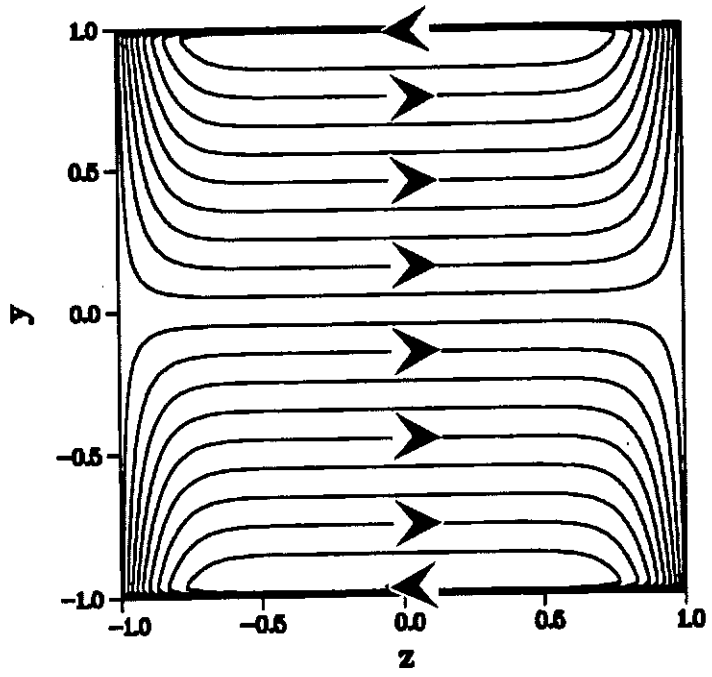

Fig. 3f

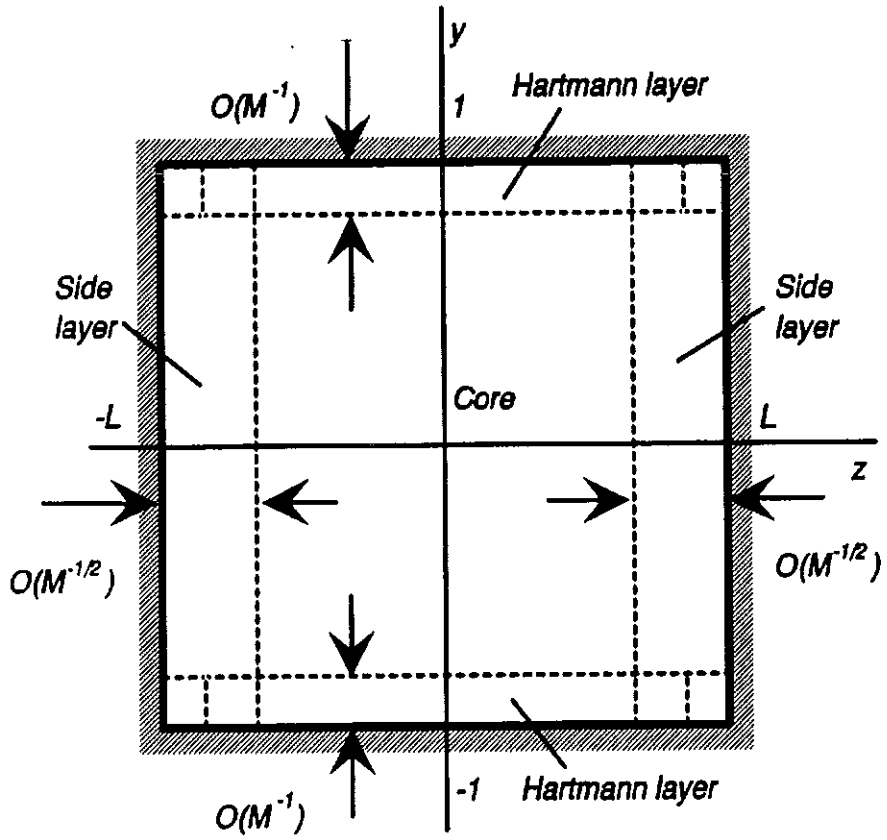

Fig. 3g

Fig. 3. For legend see previous page.

Vatazhin, Liubimov & Regirer (1970) present an asymptotic expansion of the pressure gradient in powers of $M^{-\frac{1}{2}}$, namely

$$k = \frac{1}{M}\left\{1 - \frac{0.852}{L\sqrt{M}} - \frac{1}{M}\right\}, \qquad (4)$$

which has been obtained using Shercliff's asymptotic solution. The expression (4) may be used for calculating pressure drop in straight insulating rectangular ducts for $M>10$ with the error of less than 10%, while even more simple expression

$$k = M^{-1} \qquad (5)$$

may be used for $M>100$ with the same accuracy (Fig. 4).

More sophisticated fully developed flows with magnetic field inclined to the duct walls, or with non-perfect insulation of the duct walls have been considered by Vatazhin, Liubimov & Regirer (1970), Molokov (1990), Molokov & Shishko (1993) and Bühler & Molokov (1993).

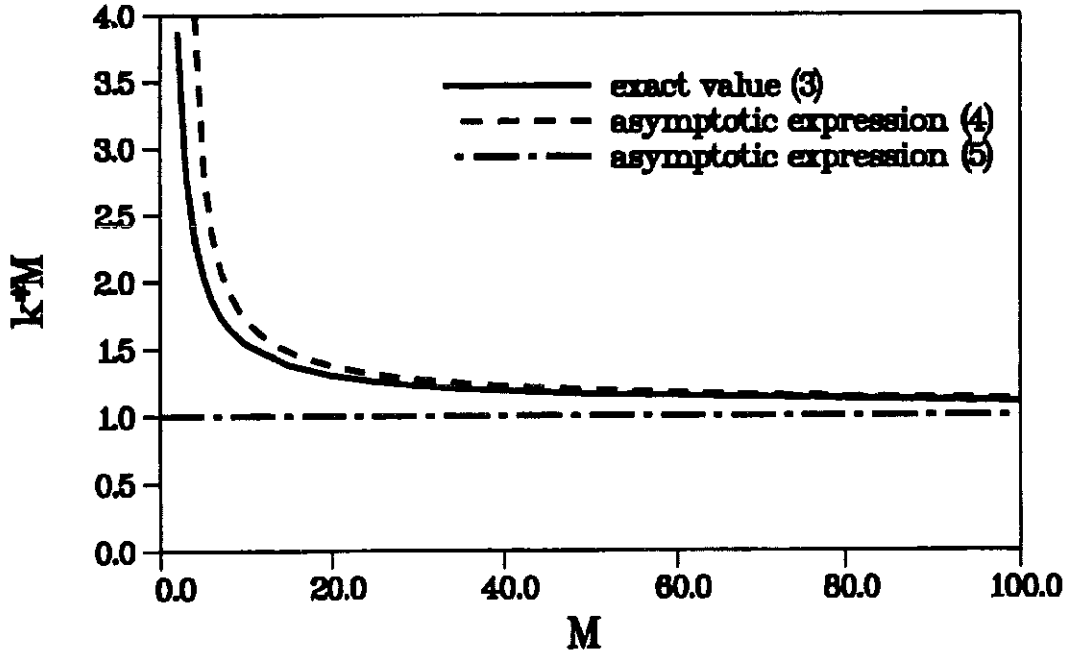

Fig. 4 Variation of the pressure gradient in a straight insulating square duct (L=1) with the Hartmann number.

The behaviour of the Shercliff's solution at high M justifies the application of the asymptotic theory to general 3-D flows in ducts. The general inertialess three-dimensional flow in a duct of arbitrary shape of the Hartmann walls but with no side walls has been treated by Kulikovskii (1968) and Hunt & Ludford (1968). Neglecting inertia terms in the core and in the Hartmann layers requires only that $N>>1$. Neglecting also viscous terms for $M>>1$,

Kulikovskii and Hunt & Ludford reduce the three-dimensional problem (1) to a number of two-dimensional equations for the core potential and the pressure. The solution to the resulting equations depends on the duct geometry.

Three-dimensional flows in insulating ducts of finite cross-section have been considered first by Walker, Ludford & Hunt (1972) (hereinafter referred to as WLH), who treat the inertialess flow in a symmetric expansion of the rectangular duct in the plane of the magnetic field, while the side walls are parallel to each other. They present asymptotic solution to the flow in a straight duct connected to the linear expansion and show that in the core of the expanding duct the fluid is virtually stagnant with the magnitude of the velocity $O(M^{-\frac{1}{2}})$, while all volume flux is carried by the high-velocity jets at the side walls. The velocity in the jets is $O(M^{\frac{1}{2}})$. The three-dimensional disturbance caused by the expansion extends into the straight duct to the distances *O(1)*, i. e. the disturbance dies out at about one characteristic length from the join of the expansion and the straight duct. The magnitude of the transverse electric currents due to the expansion (3-D currents) is $O(M^{-\frac{1}{2}})$, and thus the 3-D pressure drop produced by these currents is $O(M^{-\frac{1}{2}})$. Since in fully developed flow the pressure gradient is $O(M^{-1})$, for $M\sim10^4$ the 3-D pressure drop is approximately two orders higher than the 2-D one for a straight duct per unit length, so that 3-D effects in insulating ducts expanding in the plane of the field are significant. The same effects as those in duct expansions are present in flows in straight ducts with nonuniform magnetic field varying in the flow direction (Lavrentiev *et al.* 1990). It is very important to note that the presence of the side walls radically changes the range of validity of the inertialess approximation in flows of WLH and Lavrentiev *et al.* from $N>>1$ to $N >> M^{\frac{3}{2}}$, the latter being hardly realised in practice. However, there is a belief that apart from (quasi-) two-dimensional turbulence (Moreau 1990, Chap. VII), which may be present in the core and produce negligible additional pressure drop, inertia effects really affecting the pressure drop are confined to the side layers (cf. experiments by Picologlou & Reed, 1989).

Strong 3-D effects in the flow of WLH are caused by the expansion in the field direction. In the present investigation a different case of parallel top and bottom walls is considered, while the variation of the duct cross section occurs in the plane (x,z) perpendicular to the magnetic field. In this case, as has been noted in concluding remarks by WLH, there is no considerable three-dimensional effect. The side layers do not carry *O(1)* volume flux and the core is not stagnant. We present the analysis of the flow in several geometries due to their importance in blanket-relevant research. In Sec. 4 the analysis generally follows that of WLH. It is extended to obtain second terms in the asymptotic expansions in powers of $M^{-\frac{1}{2}}$, since they determine the pressure drop. The flow structure in the core is valid for $N>>1$, $M>>1$; both assumptions hold for all self-cooled blanket concepts, while the effects of inertia in the side layers and their influence on the pressure drop are discussed in Sec. 6.

4. Flow analysis at large Hartmann numbers

For convenience, in this section we refer to the flow in a symmetric 180°-turn (Fig. 5a), while the generalisation of the analysis to other geometries is discussed at the end of the Section. Flow subregions at high Hartmann number in a 180°-turn in the plane *(x,z)* are shown in Fig. 5b.

At the first stage the Hartmann layers at the walls $y = \pm 1$ are excluded from the analysis, provided the core- and the side-layer- variables satisfy the conditions

$$v = M^{-1}\left\{\frac{\partial u}{\partial x} + \frac{\partial w}{\partial z}\right\}, \quad j_y = \pm M^{-1}\left\{\frac{\partial u}{\partial z} - \frac{\partial w}{\partial x}\right\} \qquad \text{at } y = \pm 1. \qquad (6a,b)$$

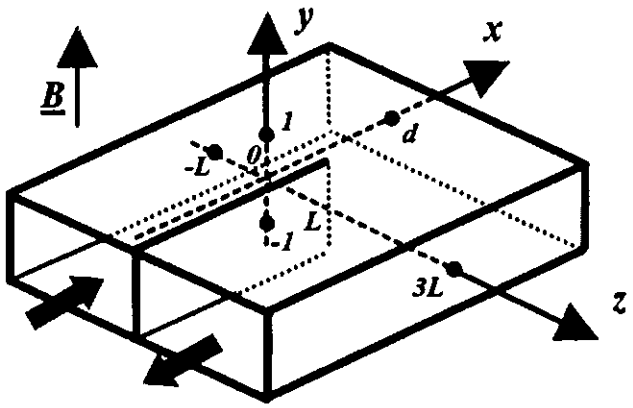

Fig. 5a

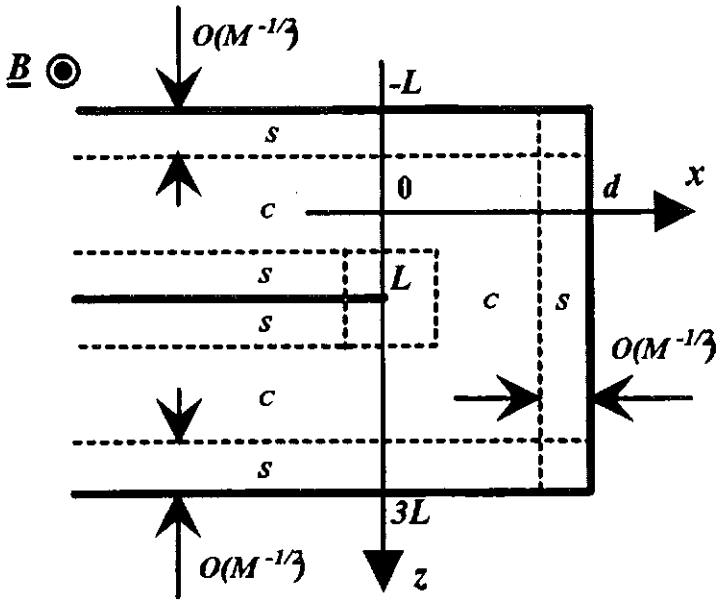

Fig. 5b

Fig. 5 Flow in a symmetric 180°-turn. **a)** flow scheme; **b)** flow subregions in the *(x,z)* plane at high Hartmann number: *C* - the core, *S* - the side layers. Corner and edge regions are unimportant for the analysis.

4. 1 Core regions

In the core of the duct the main terms in the asymptotic expansions of the flow variables are

$$\phi = \Phi^{(0)} + M^{-\frac{1}{2}}\Phi^{(\frac{1}{2})}+\ldots, \qquad p = M^{-\frac{1}{2}}P^{(\frac{1}{2})} + M^{-1}P^{(1)}\ldots, \qquad (7a,b)$$

$$u = U^{(0)} + M^{-\frac{1}{2}}U^{(\frac{1}{2})}+\ldots, \qquad w = W^{(0)} + M^{-\frac{1}{2}}W^{(\frac{1}{2})}+\ldots, \qquad (7c,d)$$

$$j_x = M^{-\frac{1}{2}}J_x^{(\frac{1}{2})} + M^{-1}J_x^{(1)}+\ldots, \qquad j_z = M^{-\frac{1}{2}}J_z^{(\frac{1}{2})} + M^{-1}J_z^{(1)}+\ldots. \qquad (7e,f)$$

Upper indices $^{(i)}$ denote coefficients in the asymptotic expansions at M^{-i}. Capital letters denote the core variables.

The y-components of the fluid velocity v and of the electric current density j_y vanish at least to the order $M^{-\frac{1}{2}}$ and thus are unimportant for the analysis. The x- and z- components of the fluid velocity and the electric current are expressed in terms of the electric potential and the pressure as follows

$$U^{(0,\frac{1}{2})} = \frac{\partial\Phi^{(0,\frac{1}{2})}}{\partial z}, \qquad W^{(0,\frac{1}{2})} = -\frac{\partial\Phi^{(0,\frac{1}{2})}}{\partial x}, \qquad (7g,h)$$

$$J_x^{(\frac{1}{2},1)} = \frac{\partial P^{(\frac{1}{2},1)}}{\partial z}, \qquad J_z^{(\frac{1}{2},1)} = -\frac{\partial P^{(\frac{1}{2},1)}}{\partial x}. \qquad (7i,j)$$

The $O(1)$ and $O(M^{-\frac{1}{2}})$ core electric potential and the $O(M^{-\frac{1}{2}})$ and $O(M^{-1})$ core pressure are stream functions for the fluid velocity and the electric current in the plane perpendicular to the magnetic field. They are two-dimensional harmonic functions, i. e. they satisfy the Laplace equations

$$\frac{\partial^2\Phi^{(i)}}{\partial x^2} + \frac{\partial^2\Phi^{(i)}}{\partial z^2} = 0, \qquad i=0, \tfrac{1}{2}, \qquad (8a)$$

$$\frac{\partial^2 P^{(i)}}{\partial x^2} + \frac{\partial^2 P^{(i)}}{\partial z^2} = 0, \qquad i=\tfrac{1}{2},1. \qquad (8b)$$

Thus, the flow in the core is the potential flow. The boundary conditions for the functions $\Phi^{(i)}(x,z)$ and $P^{(i)}(x,z)$ are the conditions of matching with the side-layer solutions and the conditions of fully developed flow far from the joins between ducts and from the duct expansions. Then the conditions at $x \to -\infty$ are

$$\frac{\partial \Phi^{(0,1/2)}}{\partial x} \to 0, \quad P^{(1/2)} \to 0, \quad \frac{\partial P^{(1)}}{\partial x} \to -1 \qquad \text{as } x \to -\infty. \qquad (8c\text{-}f)$$

Since the flow is inertialess, the conditions at the symmetry plane are

$$P^{(i)} = 0, \qquad i=\tfrac{1}{2},1, \qquad (8g,h)$$

at $z=L$, $0 \le x \le d$

$$\frac{\partial \Phi^{(i)}}{\partial z} = 0, \qquad i=0,\ \tfrac{1}{2}. \qquad (8i,j)$$

The conditions at $z = \pm L$ and at $x=d$ for the core potential and the pressure require consideration of the side layers.

4. 2 Side layer at z=-L

Introducing the variable $\varsigma = \sqrt{M}(z+L)$ stretches the vicinity of the side wall $z=-L$. In the side layer the main terms in the asymptotic expansions of the flow variables are

$$\phi_S = \phi_S^{(0)} + M^{-\frac{1}{2}}\phi_S^{(1/2)} + \ldots, \qquad p_S = M^{-\frac{1}{2}}p_S^{(1/2)} + M^{-1}p_S^{(1)} \ldots, \qquad (9a,b)$$

$$u_S = M^{\frac{1}{2}}u_S^{(-1/2)} + u_S^{(0)} + \ldots, \qquad v_S = M^{\frac{1}{2}}v_S^{(-1/2)} + v_S^{(0)} + \ldots, \qquad (9c,d)$$

$$w_S = w_S^{(0)} + M^{-\frac{1}{2}}w_S^{(1/2)} + \ldots, \qquad j_{x,S} = j_{x,S}^{(0)} + M^{-\frac{1}{2}}j_{x,S}^{(1/2)} + \ldots \qquad (9e,f)$$

$$j_{y,S} = j_{y,S}^{(0)} + M^{-\frac{1}{2}}j_{y,S}^{(1/2)} + \ldots, \qquad j_{z,S} = M^{-\frac{1}{2}}j_{z,S}^{(1/2)} + M^{-1}j_{z,S}^{(1)} + \ldots. \qquad (9g,h)$$

The problems for the first two terms in the asymptotic expansions of the side-layer variables are

$$\frac{\partial^2 u_S^{(-1/2,0)}}{\partial \varsigma^2} - j_{z,S}^{(1/2,1)} = \frac{\partial p_S^{(1/2,1)}}{\partial x}, \qquad (10a)$$

$$\frac{\partial^2 v_S^{(-1/2,0)}}{\partial \varsigma^2} = \frac{\partial p_S^{(1/2,1)}}{\partial y}, \qquad (10b)$$

$$j_{x,S}^{(0,1/2)} = \frac{\partial p_S^{(1/2,1)}}{\partial \varsigma}, \qquad (10c)$$

$$j_{x,S}^{(0,1/2)} = -\frac{\partial \phi_S^{(0,1/2)}}{\partial x} - w_S^{(1/2,1)}, \qquad (10d)$$

$$j_{y,S}^{(0,1/2)} = -\frac{\partial \phi_S^{(0,1/2)}}{\partial y}, \qquad (10e)$$

$$u_S^{(-1/2,0)} = \frac{\partial \phi_S^{(0,1/2)}}{\partial \varsigma}, \qquad (10f)$$

$$\frac{\partial j_{x,S}^{(0,1/2)}}{\partial x} + \frac{\partial j_{y,S}^{(0,1/2)}}{\partial y} + \frac{\partial j_{z,S}^{(1/2,1)}}{\partial \varsigma} = 0, \qquad (10g)$$

$$\frac{\partial u_S^{(-1/2,0)}}{\partial x} + \frac{\partial v_S^{(-1/2,0)}}{\partial y} + \frac{\partial w_S^{(1,1/2)}}{\partial \varsigma} = 0. \qquad (10h)$$

The conditions at the wall $z=-L$ resulting from the conditions (1e,f) are

$$\frac{\partial \phi_S^{(0,1/2)}}{\partial \varsigma} = 0, \qquad v_S^{(-1/2,0)} = 0, \qquad (10i,j)$$

at $\varsigma = 0$

$$\frac{\partial \phi_S^{(0,1/2)}}{\partial x} = -\frac{\partial p_S^{(1/2,1)}}{\partial \varsigma}, \qquad \frac{\partial p_S^{(1/2,1)}}{\partial x} = \frac{\partial^3 \phi_S^{(0,1/2)}}{\partial \varsigma^3}. \qquad (10k,l)$$

The mass-flux condition (1g), together with the equations (10d,f,h), gives

$$\int_{-1}^{1} \phi_S^{(0,1/2)}(x, \varsigma = 0, y)dy = -2L. \qquad (10m)$$

Equations (6a,b) give the conditions at the Hartmann wall, namely

$$v_S^{(-1/2,0)} = 0, \qquad \frac{\partial \phi_S^{(0,1/2)}}{\partial y} \mp \frac{\partial^2 \phi_S^{(0,1/2)}}{\partial \varsigma^2} = 0 \qquad \text{at } y = \pm 1. \qquad (10n)$$

The conditions of matching with the core variables and the conditions of fully developed flow far from the turn are

$$\phi_S^{(0)} \to \Phi^{(0)}, \quad \phi_S^{(1/2)} \to \Phi^{(1/2)} + \varsigma \frac{\partial \Phi^{(0)}}{\partial z}(x, z = 1),$$

$$p_S^{(1/2)} \to P^{(1/2)}, \; p_S^{(1)} \to P^{(1)} \quad \text{as } \varsigma \to \infty, \qquad (10o\text{-}r)$$

$$\frac{\partial \phi_S^{(0,1/2)}}{\partial x} \to 0, \quad p_S^{(1/2)} \to 0, \quad \frac{\partial p_S^{(1)}}{\partial x} \to -1 \text{ as } x \to -\infty. \qquad (10s\text{-}v)$$

From (10) and (8b) follows that the solution for the *O(1)* electric potential in the side layer is

$$\phi_S^{(0)} = \Phi^{(0)}(x, z = -L) = -L, \qquad (11)$$

while the first terms in the asymptotic expansions of all other variables in the side layer and the $O(M^{-\frac{1}{2}})$ core pressure $P^{(1/2)}$ vanish, so that the pressure drop in a 180°-turn is $O(M^{-1})$. The same analysis and conclusions are valid for the side layers at $z=L$ and $x=d$. This implies no jets in the side layers, so that all volume flux is carried by the core. The role of the side layers is to match the jump in the *O(1)* core velocity to the no-slip condition at the side walls. The remaining boundary conditions for the *O(1)* core potential are

$$\Phi^{(0)}(x = d, z) = -L, \qquad (12a)$$

$$\Phi^{(0)}(x, z = L) = L \qquad \text{for } x \le 0. \qquad (12b)$$

It turns out that both components of the *O(1)* core velocity may be obtained with no reference to the side layer solutions and independent of the $O(M^{-1})$ pressure drop that is necessary for pumping the liquid metal through the channel. Thus, to determine the streamlines, one has to solve the equation (8a) with the conditions (8c,i), (11) and (12a,b).

The analysis performed can be generalised to other geometries. For example, if the side walls are at $z = \pm g(x)$, *i.e.* not straight, the core still carries all volume flux, while the core electric potential $\Phi^{(0)}$ is constant along the side walls, since

$$Q = \int_{-1}^{1} dy \int_{-g(x)}^{g(x)} U^{(0)} dz = 2\left\{\Phi^{(0)}(x, z = g(x)) - \Phi^{(0)}(x, z = -g(x))\right\} = 4L, \qquad (13)$$

where Q is the flow rate. The same conclusions apply to ducts with manifolds. The potential is constant along each side wall, including the dividing walls, and the difference between side-wall potentials in each subchannel determines the flow rates.

In all these geometries 3-D pressure drop is of the same order as the pressure gradient in the fully developed flow, or equivalently, the pressure drop in a straight duct per unit length, and thus may be neglected in the first approximation. If necessary, 3-D pressure drop can be determined from the solution of the coupled problem (8), (10) and (11) for the second-order

approximation for the core and the side-layer variables. We do not solve this problem here. Instead the flow structure in several basic blanket elements is discussed.

The problem consisting of the equation (8a), prescribed constant potential at the walls and the conditions of fully developed flow is solved numerically. Since the computational domain is complex, depending on the geometry being considered it is divided into several rectangular subdomains. The Laplace equation is solved in each subdomain with a Fast Poisson Solver. Iterations between solutions in subdomains are organised until continuity of the potential and its normal derivative holds at the joins between subdomains within specified accuracy. This procedure has been successfully applied to a much more complicated problem of the flow in an electrically conducting U-bend (Molokov & Bühler, 1993, 1994).

4. Flow structure in basic blanket elements

In this section the flow structure in basic blanket elements, such as elbows, expansions, manifolds, etc. is presented. The results are shown in Figs. 6-16. Although the flow geometries are different, there are certain common features. The figures indicate that the developing length, i.e the distance from the edges, corners, etc. where slug velocity profile is attained, is very short in all elements, and is roughly equal to the duct width. Peaks of velocity occur at the inner walls, and especially close to the edges, since the gradient of the electric potential is high there. At the edges the velocity may exceed the average one by the factor of 2-7, independent of the Hartmann number, provided the latter is high. This can be compared to duct expansions in the magnetic field direction, where the velocity at the side walls is proportional to $\sqrt{M}$ and may reach very high values. At the outer walls close to the corners the velocity may reduce by about 10-50%. Possible hot spots may be eliminated by rounding the corners.

Flows in ducts with manifolds (Figs. 8, 9, 11, 12) are characterised by the presence of streamlines which terminate at the edges of the dividing walls. There are also streamlines which enter one subchannel, leave it and enter one of the other subchannels in the manifold. Note that part of the fluid which feeds the duct that is closest to that supplying liquid metal to the manifold must flow very close to the edge of the dividing wall, which in inertial flow can promote instabilities and turbulence, favouring heat transfer. This effect is even more expressed if other ducts in the manifold carry major part of the volume flux (Figs. 8c, 9c).

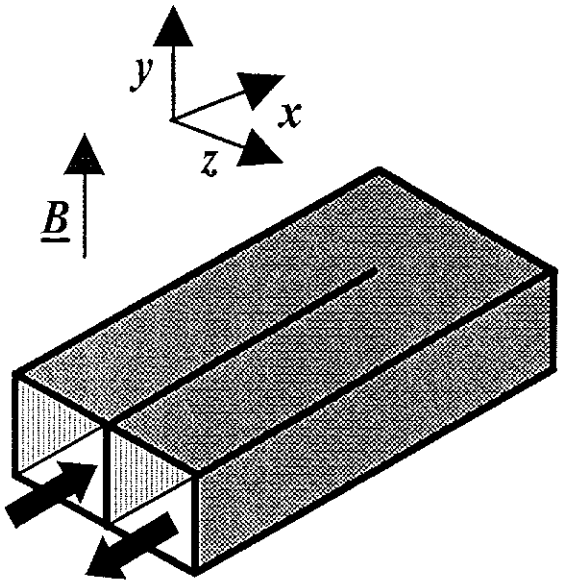

Fig. 6a

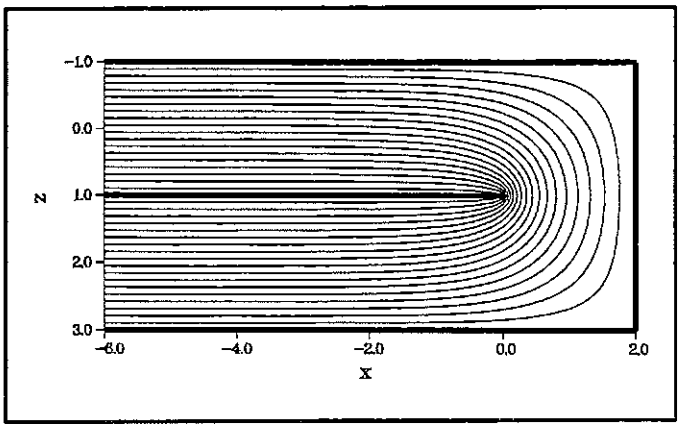

Fig. 6b

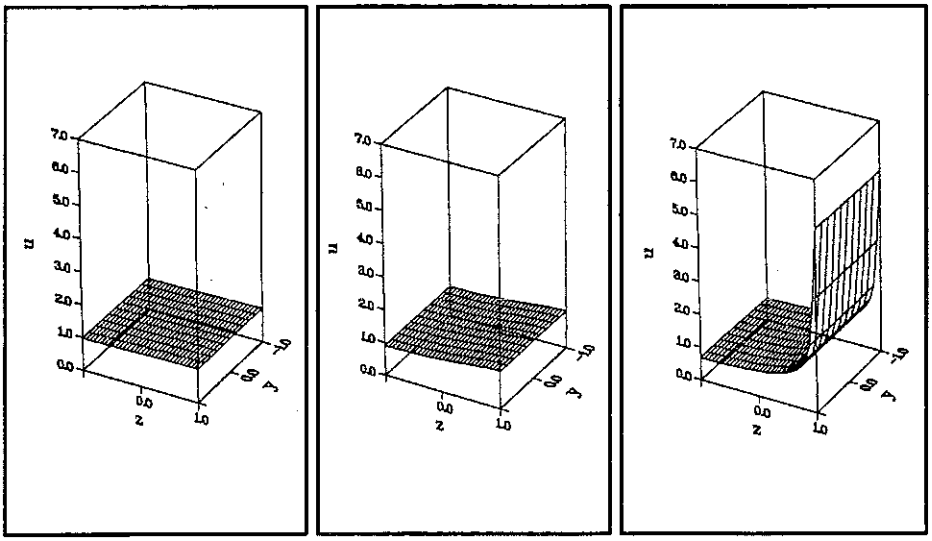

$x = -2$ $x = -1$ $x = 0$

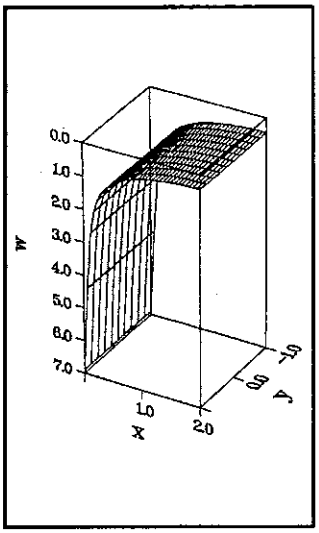

$z = 1$

Fig. 6c

Fig. 6 Flow in a symmetric 180°-turn. **a)** Flow geometry; **b)** Streamlines in the *xz* - plane; c) Development of core velocity profile.

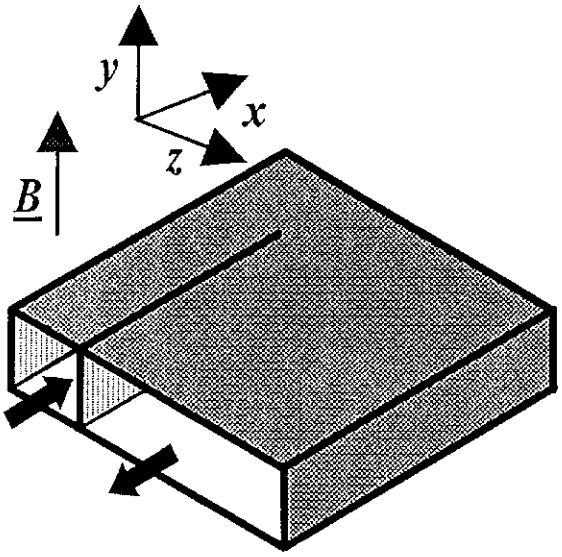

Fig. 7a

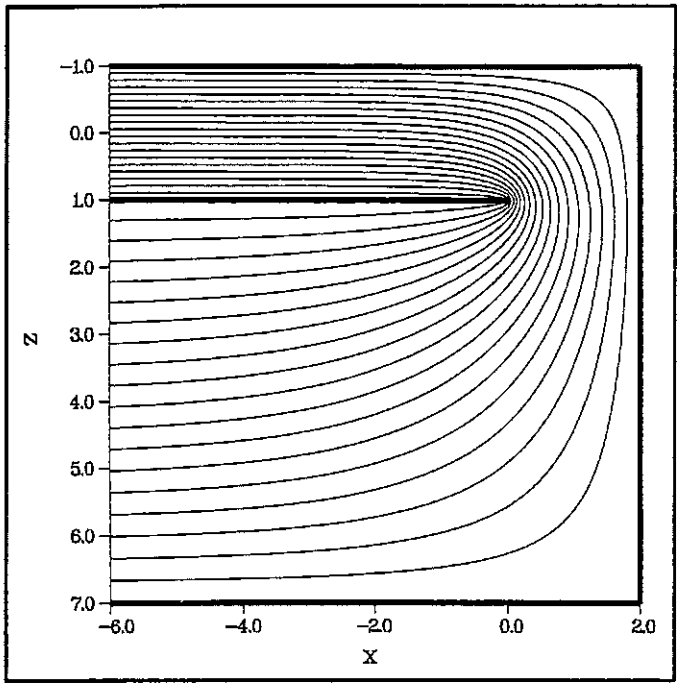

Fig. 7b

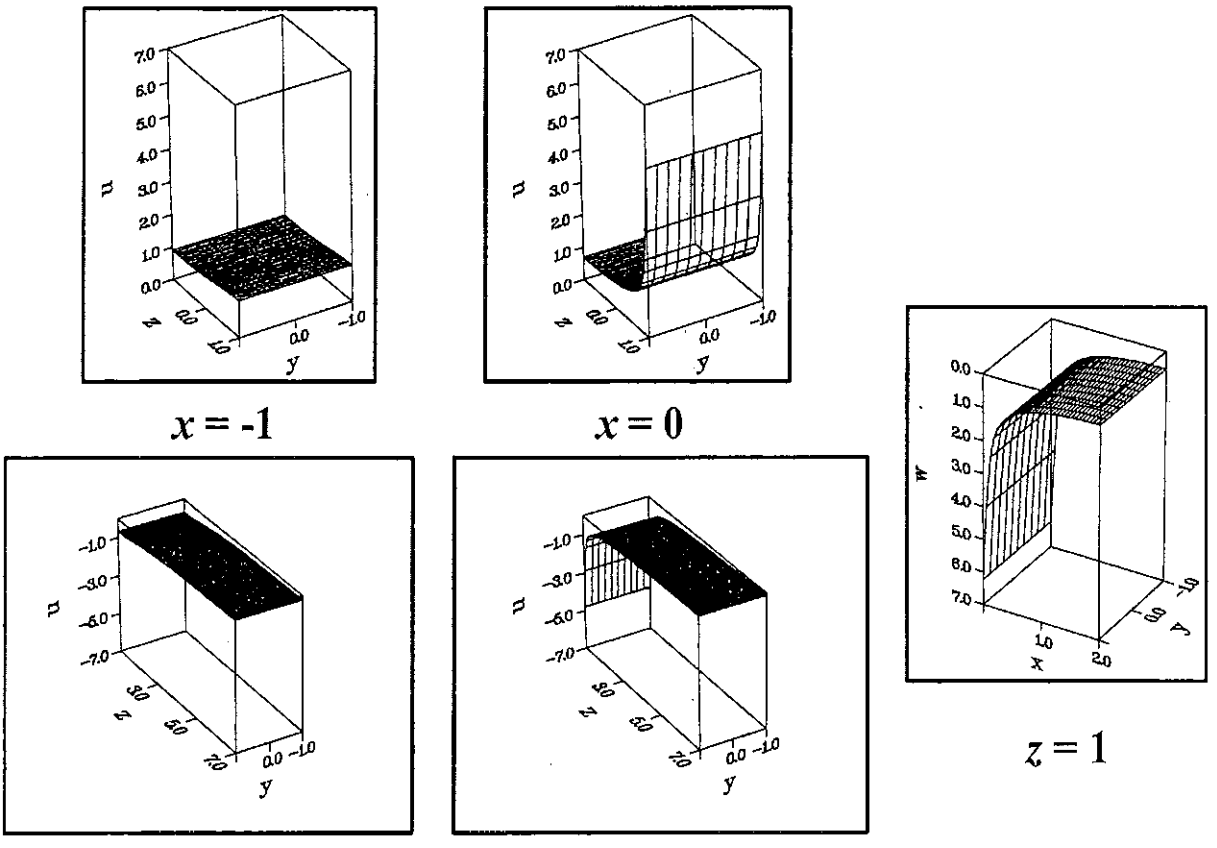

Fig. 7c

Fig. 7 Flow in a non-symmetric 180°-turn. **a)** Flow geometry; **b)** Streamlines in the *xz* - plane; **c)** Development of core velocity profile.

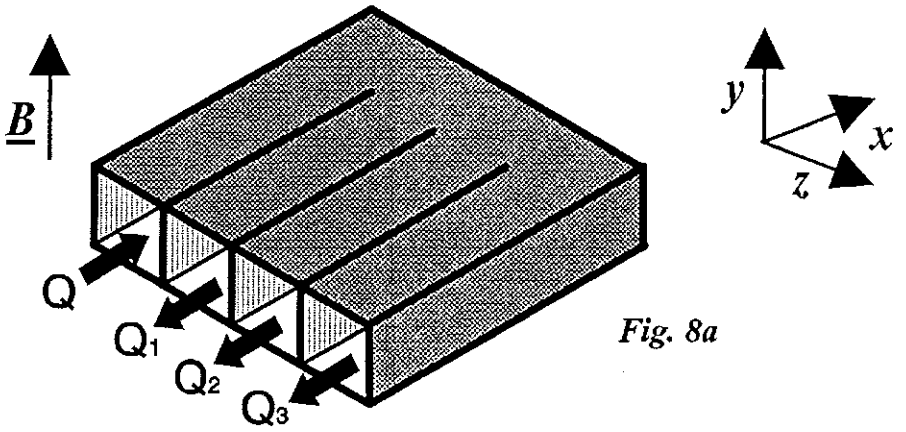

Fig. 8a

Q

$Q_1=Q/3$

$Q_2=Q/3$

$Q_3=Q/3$

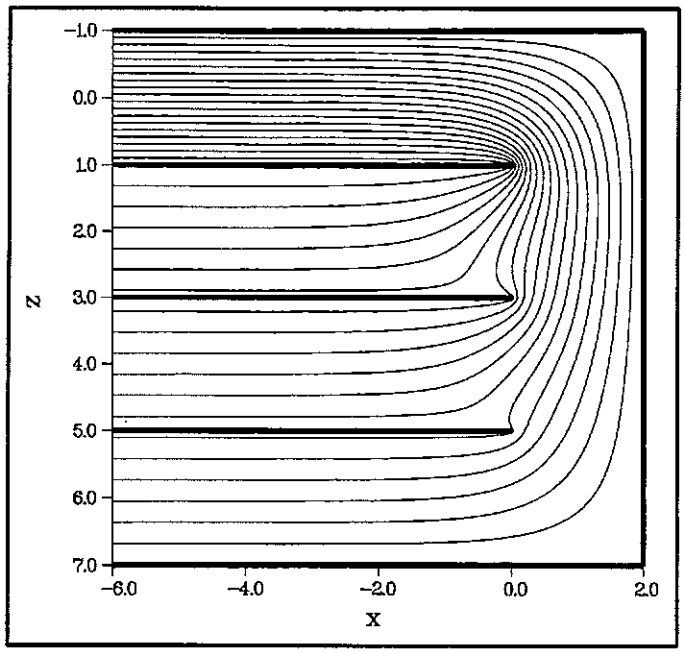

Fig. 8b

Q

$Q_1=Q/4$

$Q_2=Q/2$

$Q_3=Q/4$

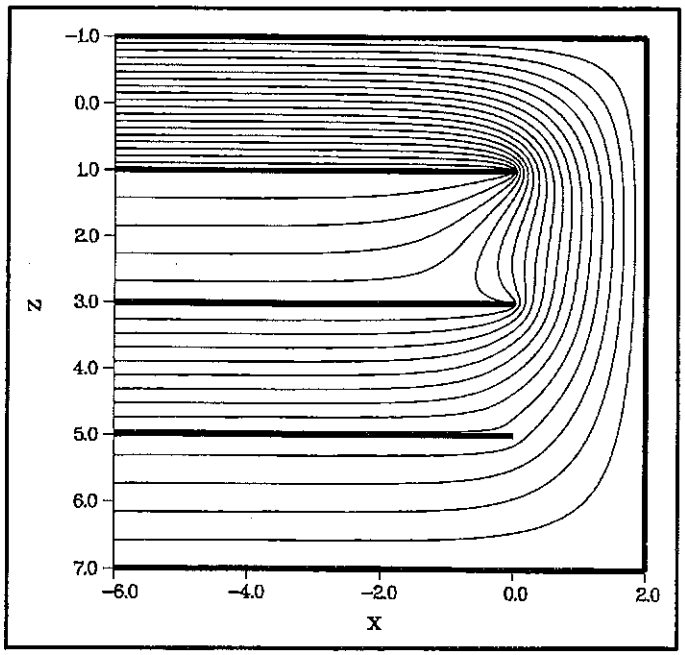

Fig. 8c

Fig. 8a-c Flow in a non-symmetric 180°-turn with manifold. **a)** Flow geometry; **b)** Streamlines in the *xz* - plane for equal flow distribution between the subchannels ($Q=3Q_1=3Q_2=3Q_3$); **c)** Streamlines in the *xz* - plane for $Q=4Q_1=2Q_2=4Q_3$.

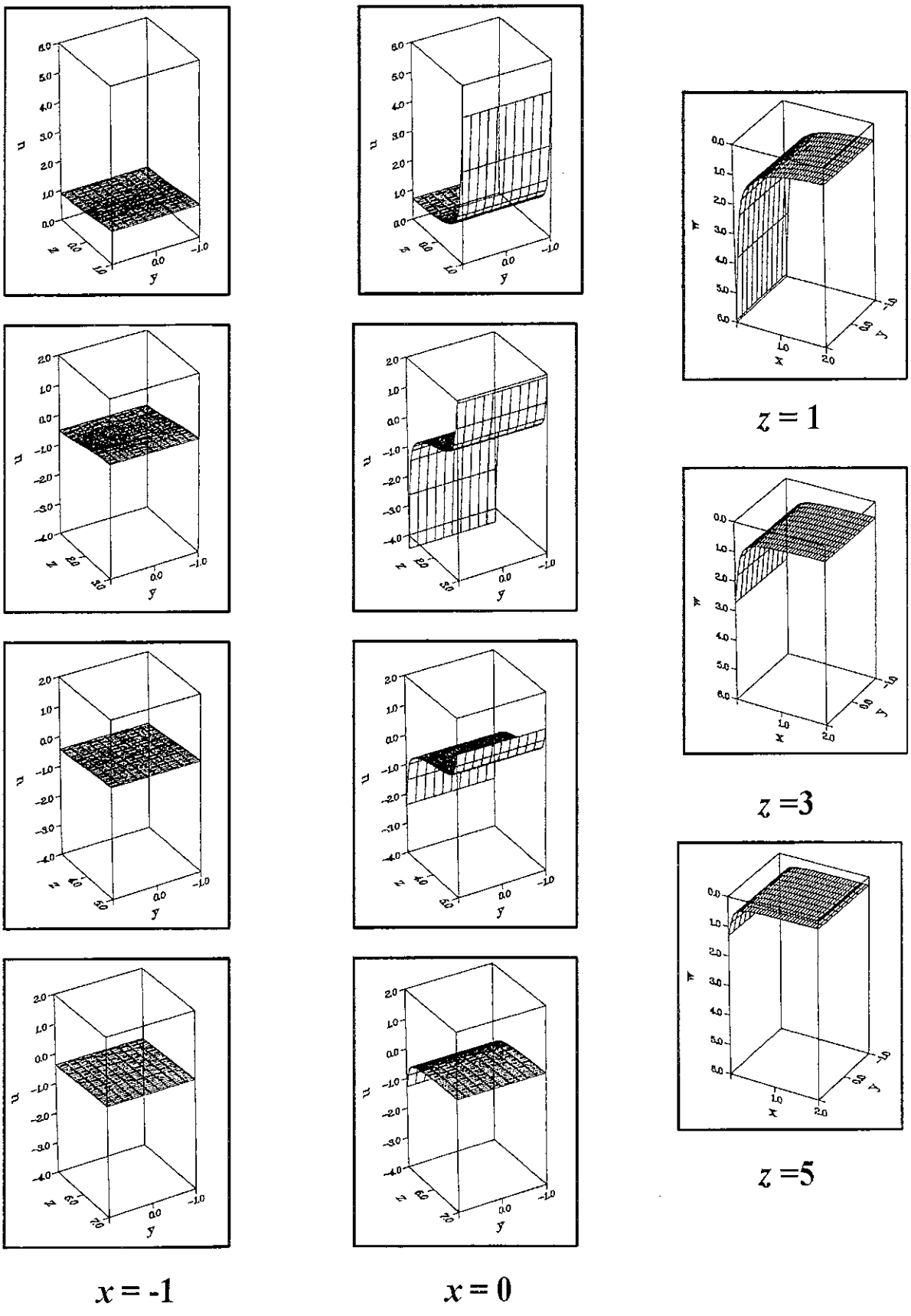

Fig. 8d Flow in a non-symmetric 180°-turn with manifold. Development of the core velocity profile for equal flow distribution between the subchannels (streamlines are shown in figure 8b).

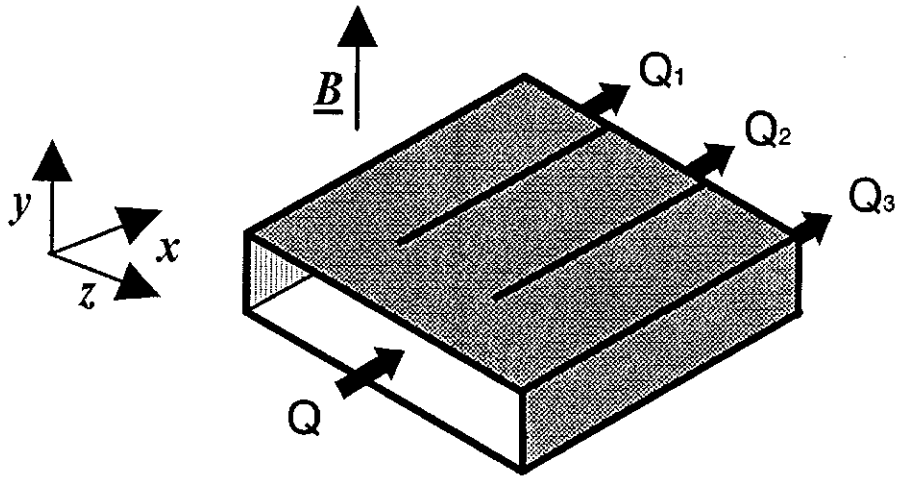

Fig. 9a

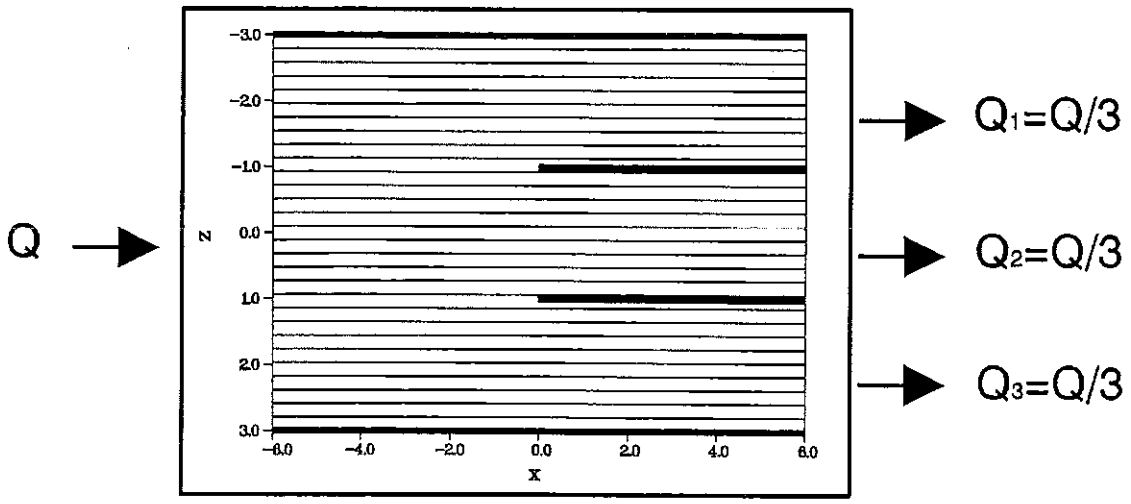

Fig. 9b

Fig. 9 Flow in a manifold distributing fluid from one straight duct to several. **a)** Flow geometry; **b-d)** Streamlines in the *xz* - plane for different flow partition between the subchannels.

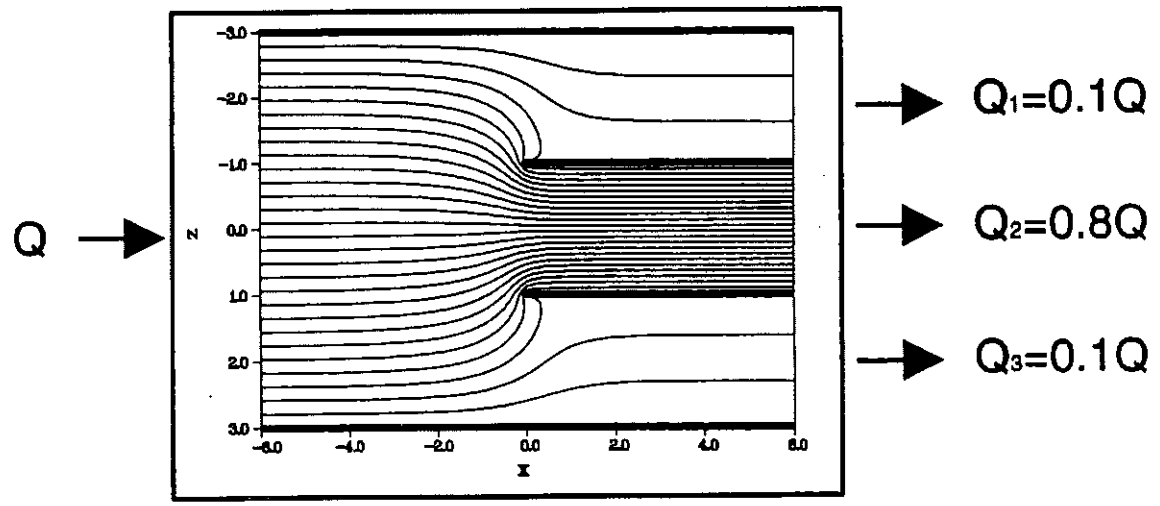

Fig. 9c

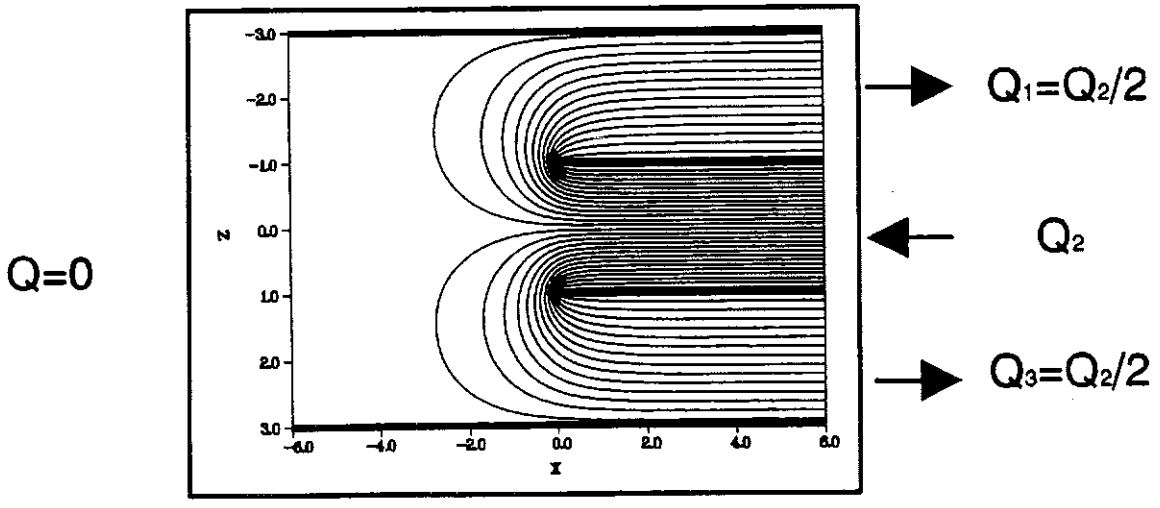

Fig. 9d

Fig. 9 For legend see previous page.

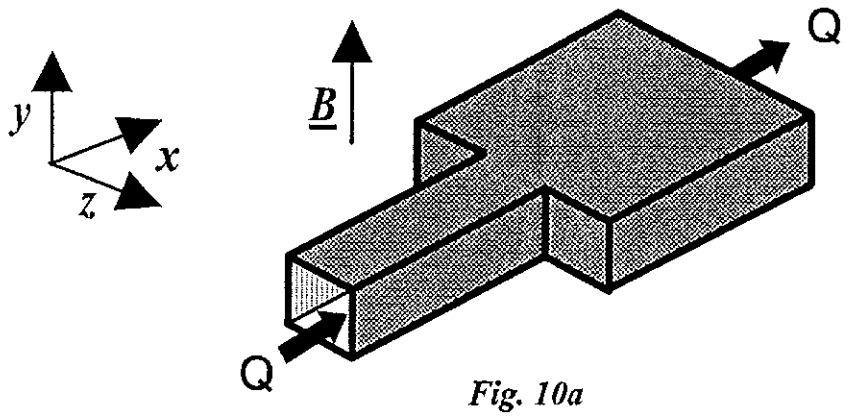

Fig. 10a

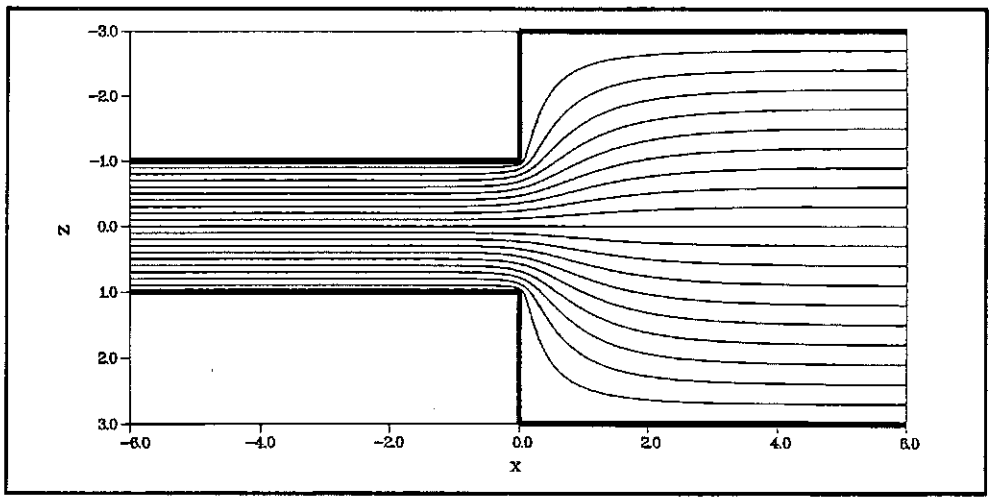

Fig. 10b

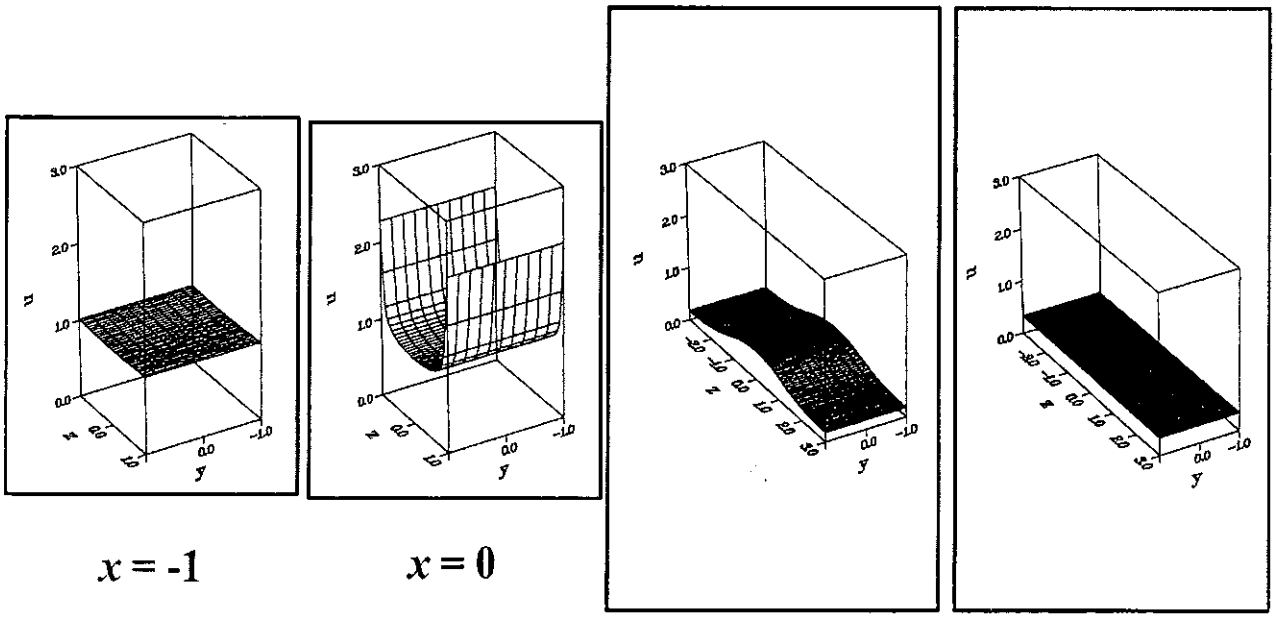

Fig. 10c

Fig. 10 Flow in a sharp expansion. **a)** Flow geometry; **b)** Streamlines in the *xz* - plane; **c)** Development of core velocity profile.

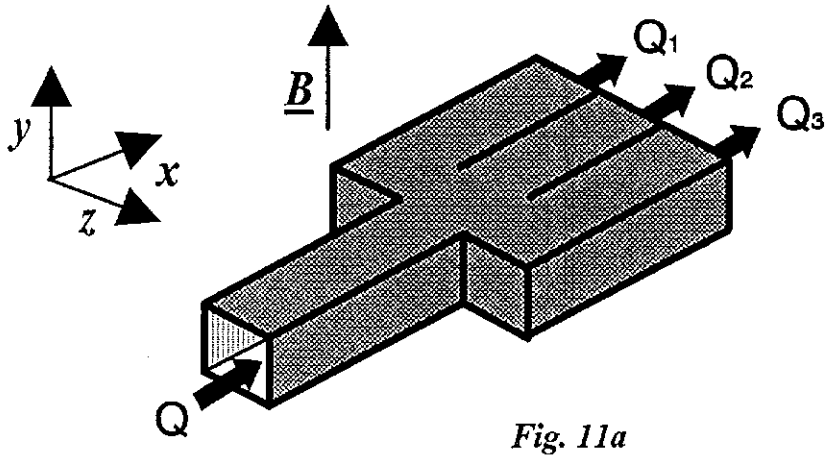

Fig. 11a

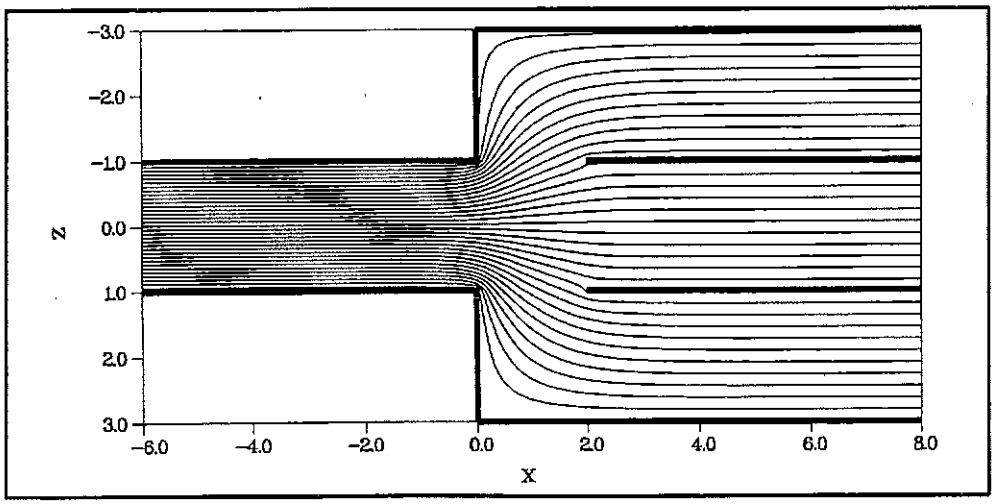

Fig. 11b

Fig. 11 Flow in a sharp expansion with manifold. **a)** Flow geometry; **b)** Streamlines in the *xz* - plane for equal flow distribution between the subchannels.

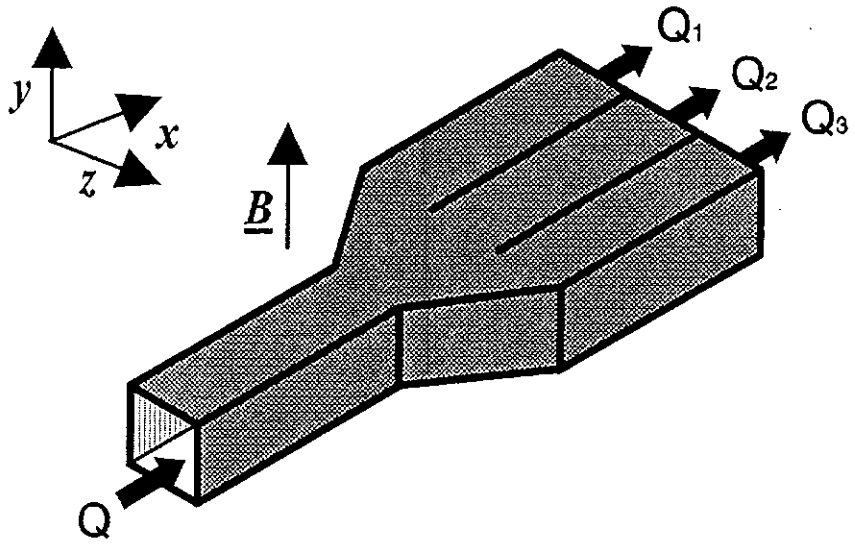

Fig. 12a

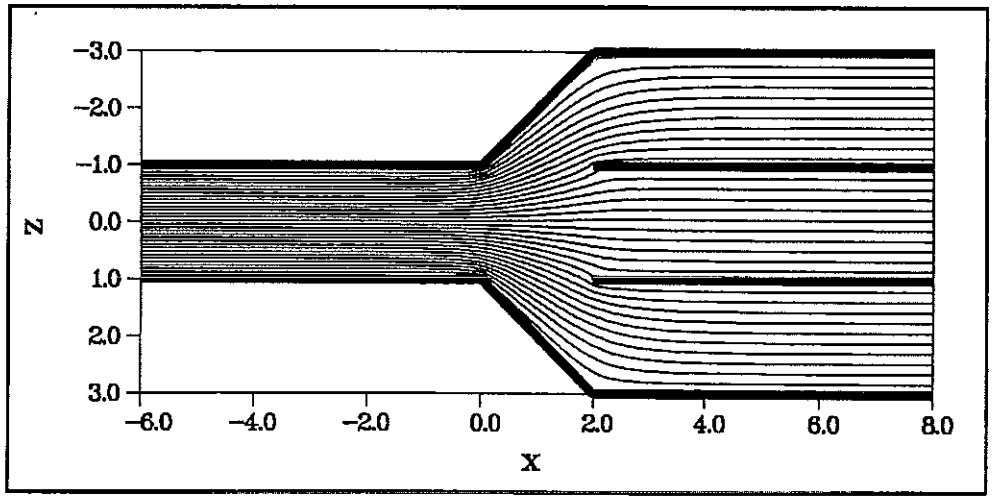

Fig. 12b

Fig. 12 Flow in a linear expansion with manifold. **a)** Flow geometry; **b)** Streamlines in the *xz* - plane for equal flow partition between the subchannels; **c)** Development of core velocity profile

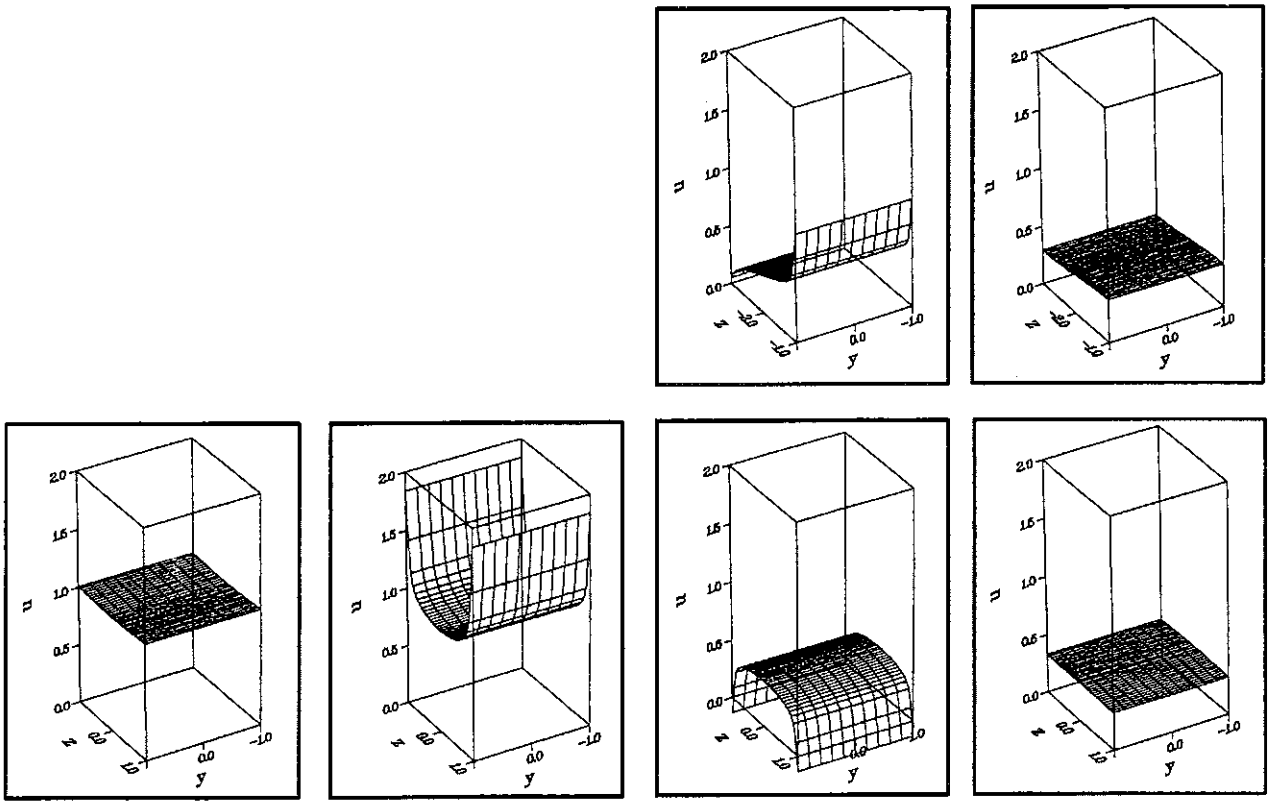

$x = -1$ $x = 0$

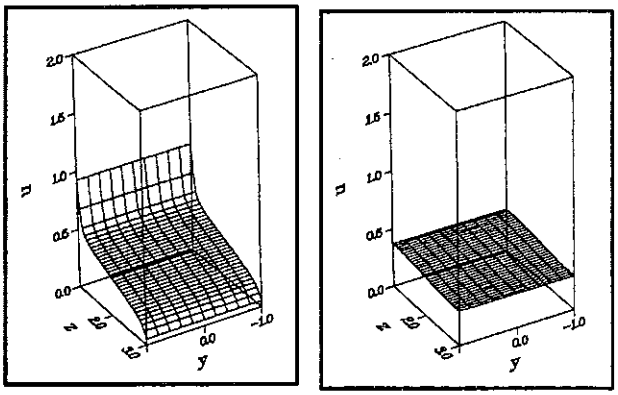

$x = 2$ $x = 3$

Fig. 12c For legend see previous page

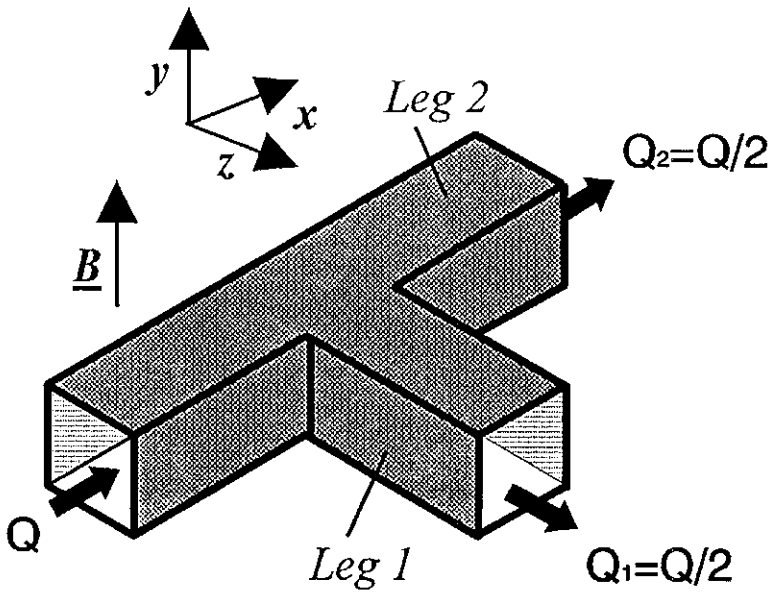

Fig. 13a

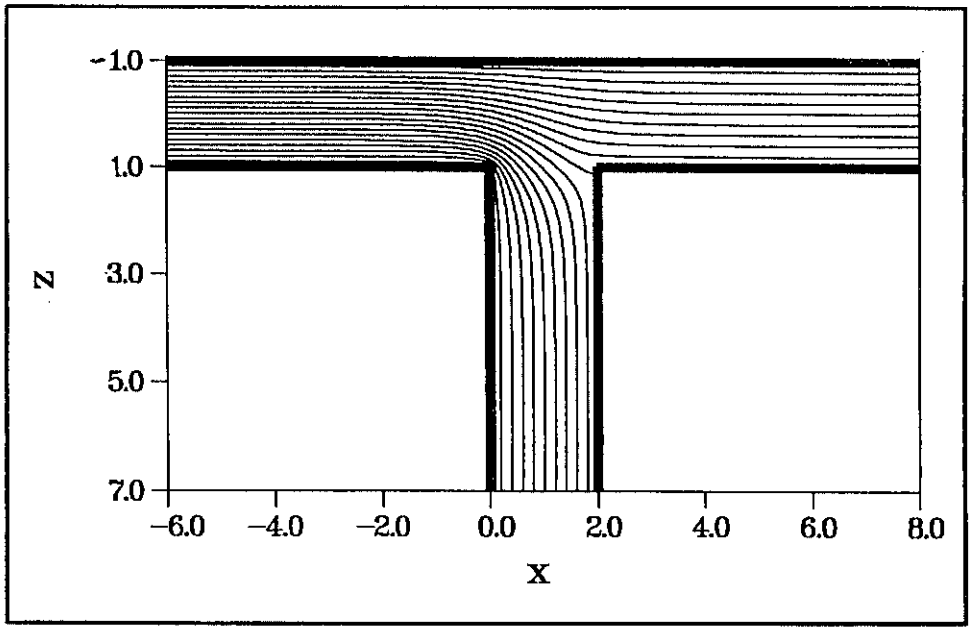

Fig. 13b

Fig. 13 Flow in a T-junction for equal flow distribution between legs 1 and 2. **a)** Flow geometry; **b)** Streamlines in the *xz*-plane; **c)** Development of the core velocity profile.

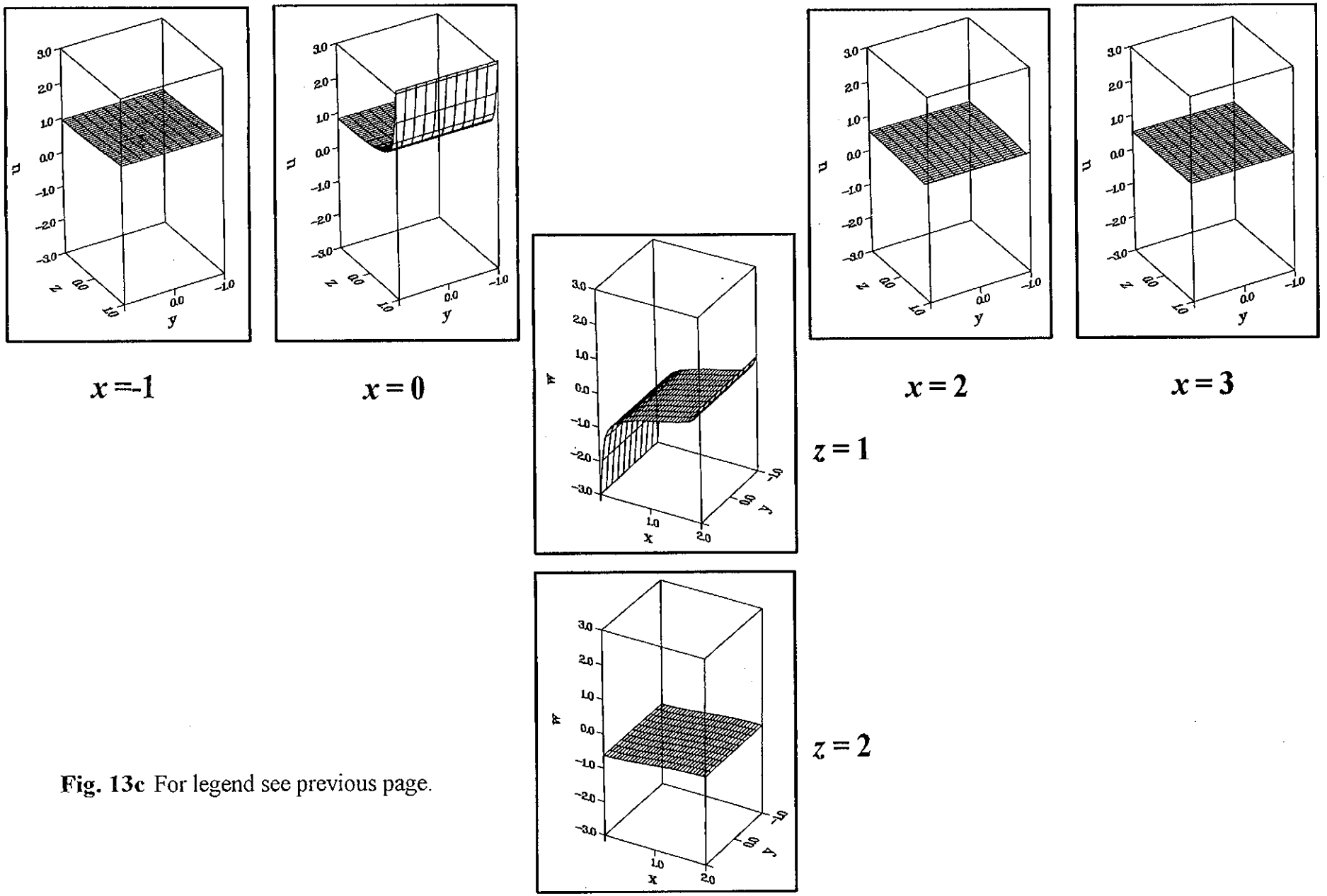

Fig. 13c For legend see previous page.

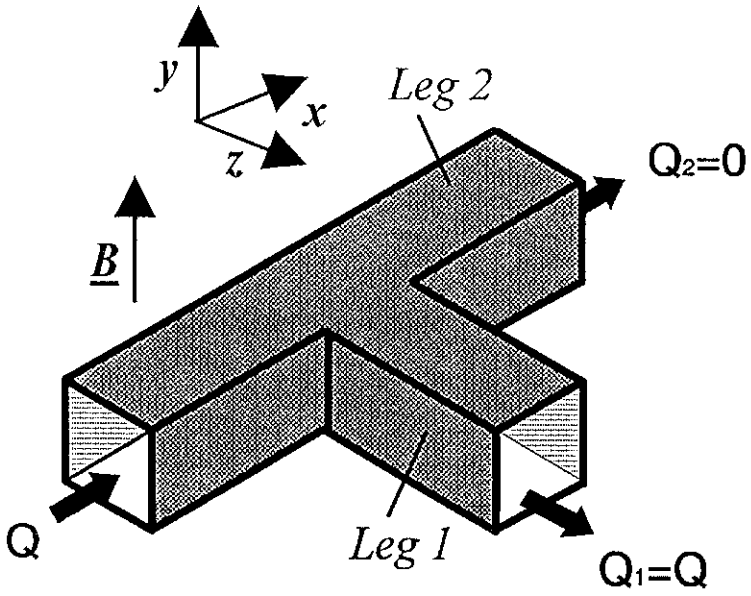

Fig. 14a

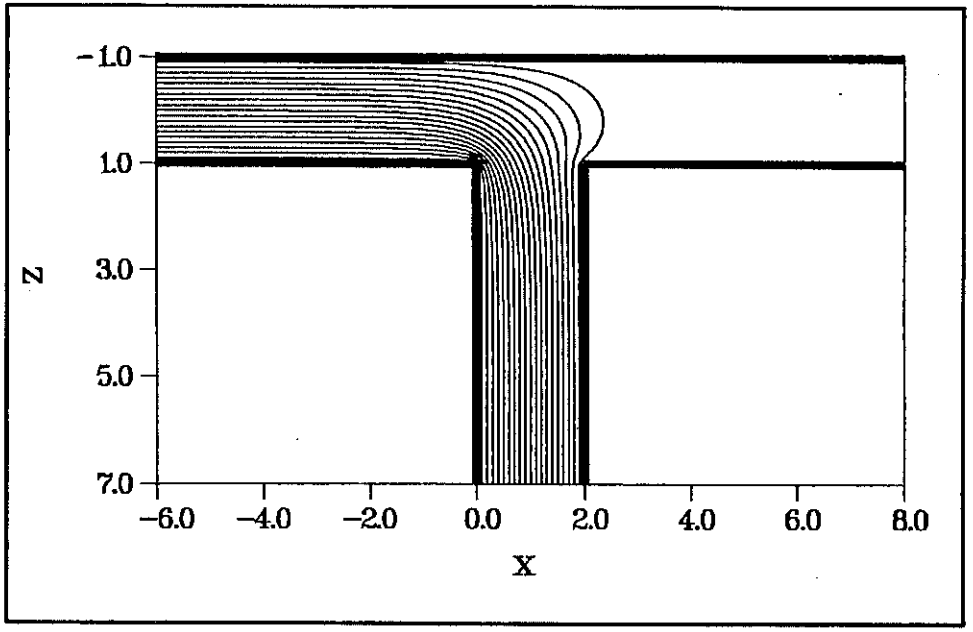

Fig. 14b

Fig. 14 Flow in a T-junction. All mass flux enters the leg 1. **a)** Flow geometry; **b)** Streamlines in the *xz*-plane; **c)** Development of the core velocity profile.

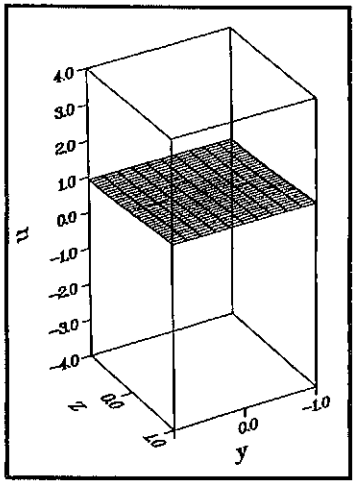

$x = -1$

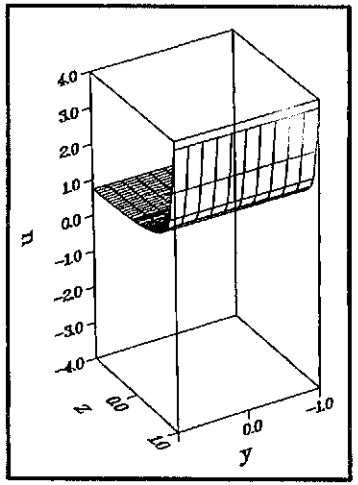

$x = 0$

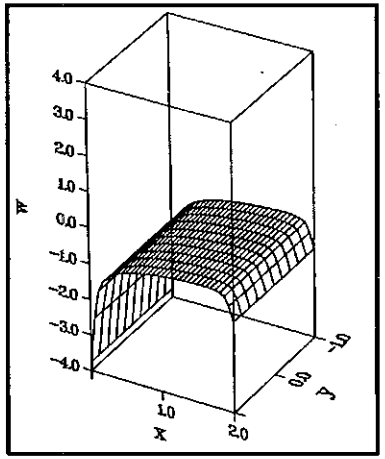

$z = 1$

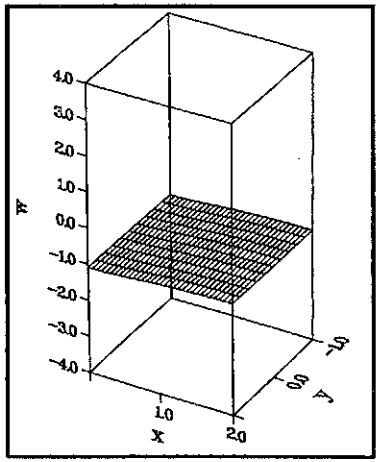

$z = 2$

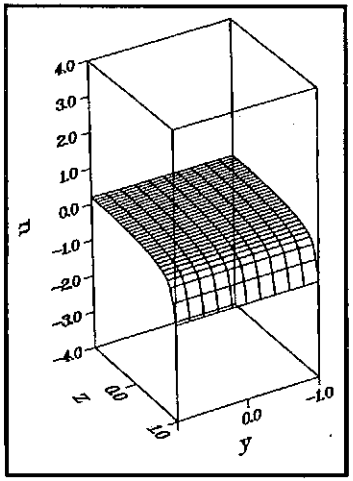

$x = 2$

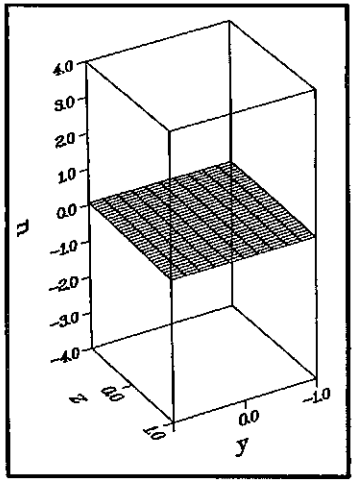

$x = 3$

Fig. 14c For legend see previous page.

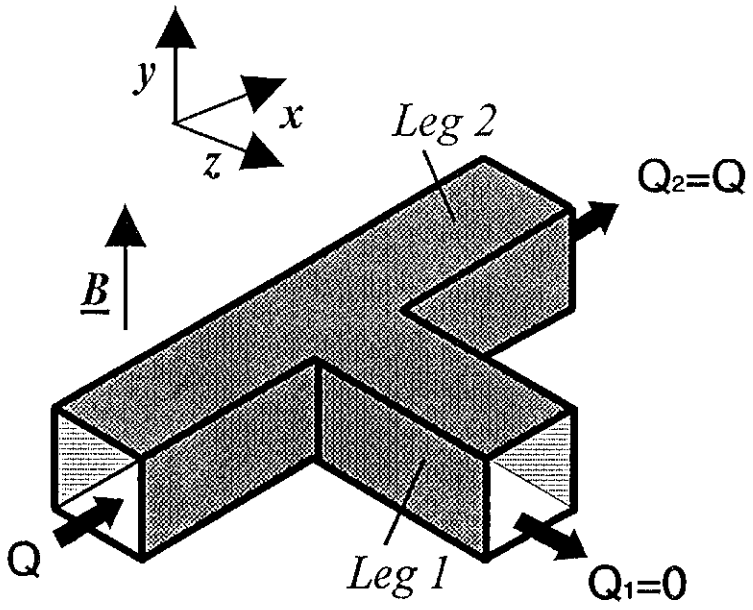

Fig. 15a

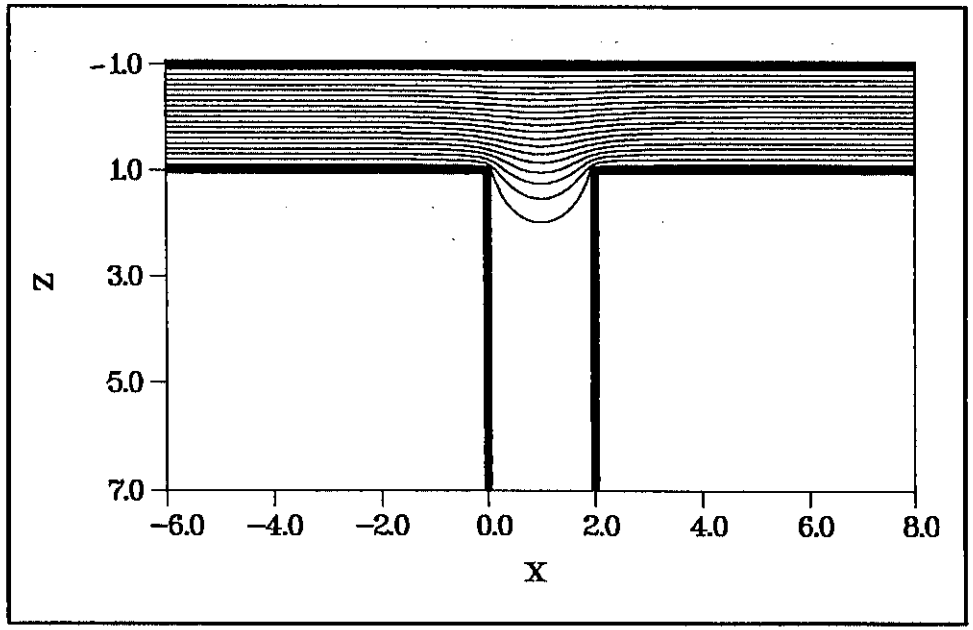

Fig. 15b

Fig. 15 Flow in a T-junction. All mass flux enters the leg 2. **a)** Flow geometry; **b)** Streamlines in the *xz*-plane; **c)** Development of the core velocity profile.

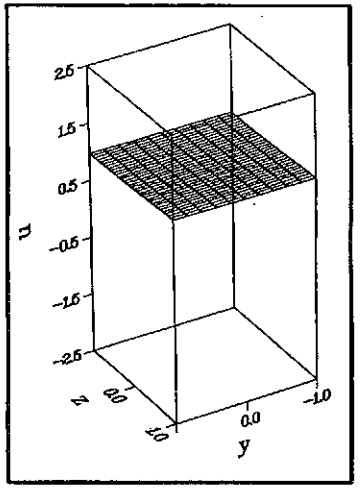

$x = -1$

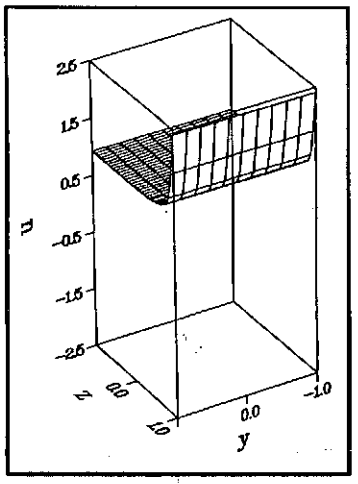

$x = 0$

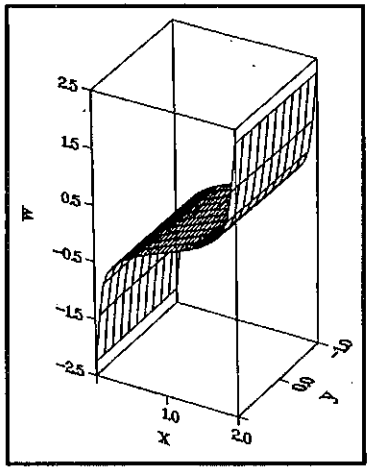

$z = 1$

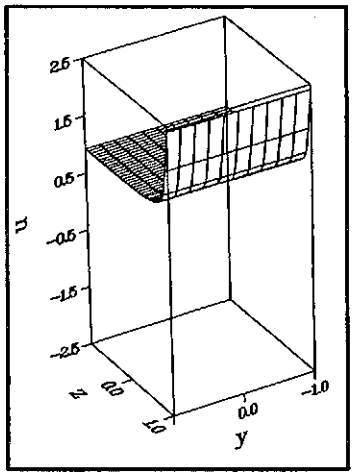

$x = 2$

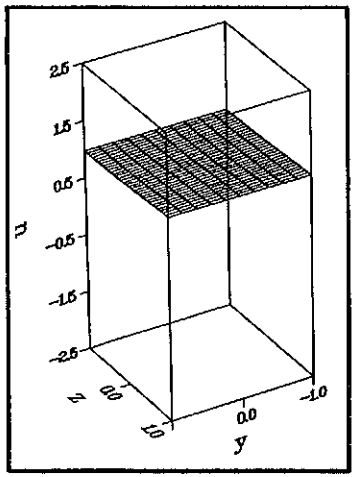

$x = 3$

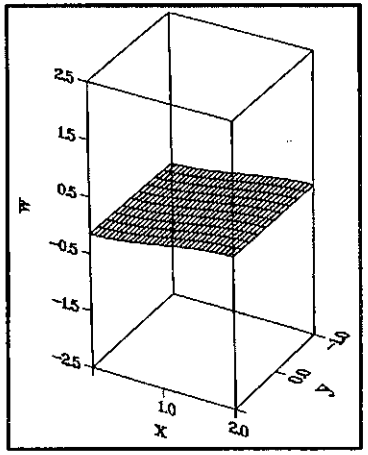

$z = 2$

Fig. 15c For legend see previous page.

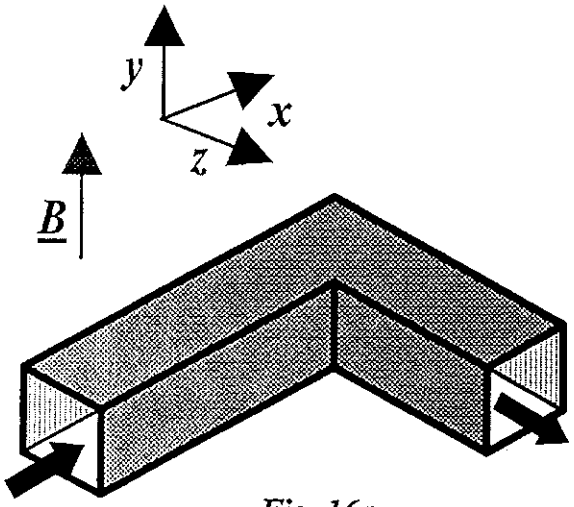

Fig. 16a

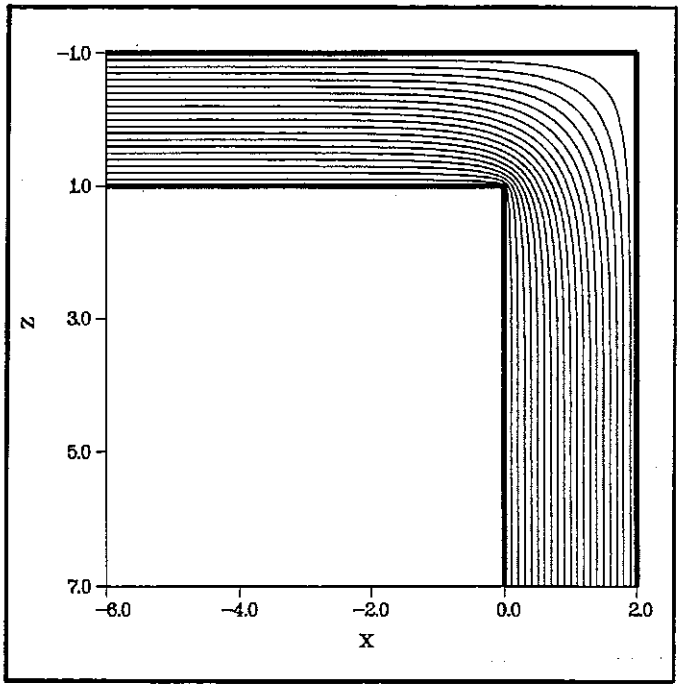

Fig. 16b

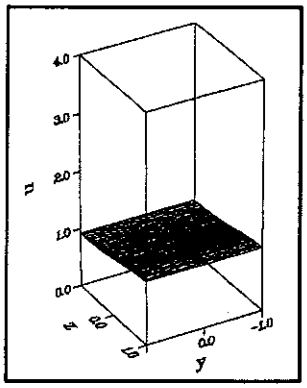

$x = -1$

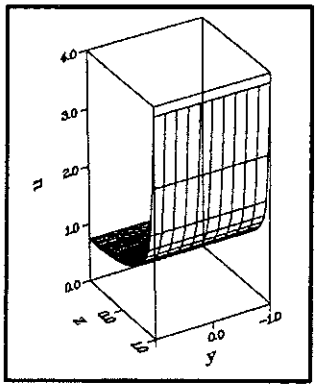

$x = 0$

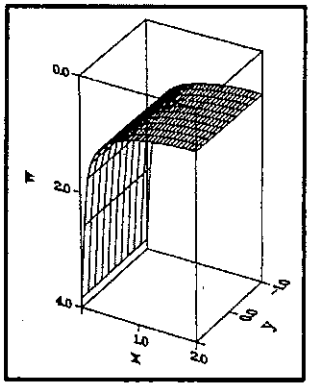

$z = 1$

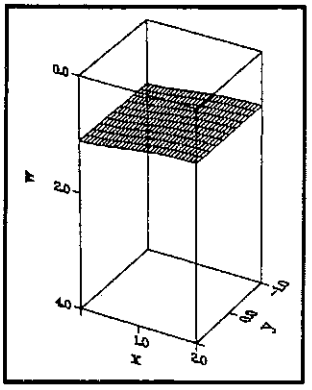

$z = 3$

Fig. 16c

Fig. 16 Flow in a sharp elbow. **a)** Flow geometry; **b)** Streamlines in the *xz* - plane; **c)** Development of core velocity profile.

The flows considered can be extended into "multi-layered" flows, one of the examples of which is shown in Fig. 17. The fluid is distributed from three channels into nine. All channels have openings into a single tank. If the flow rates in the columns are equal (uniform vertical flow distribution), there is no *O(1)* potential difference along the side walls and the flow structure is the same as in the 180°-turn with manifold (Fig. 8), so that the presence of the dividing walls perpendicular to the field is inessential. Note that the flow rates in rows may be different, as well as the number of channels in each of the columns. The latter feature may be used for creating desirable flow distribution. Obviously, this discussion can be applied to any geometry considered here.

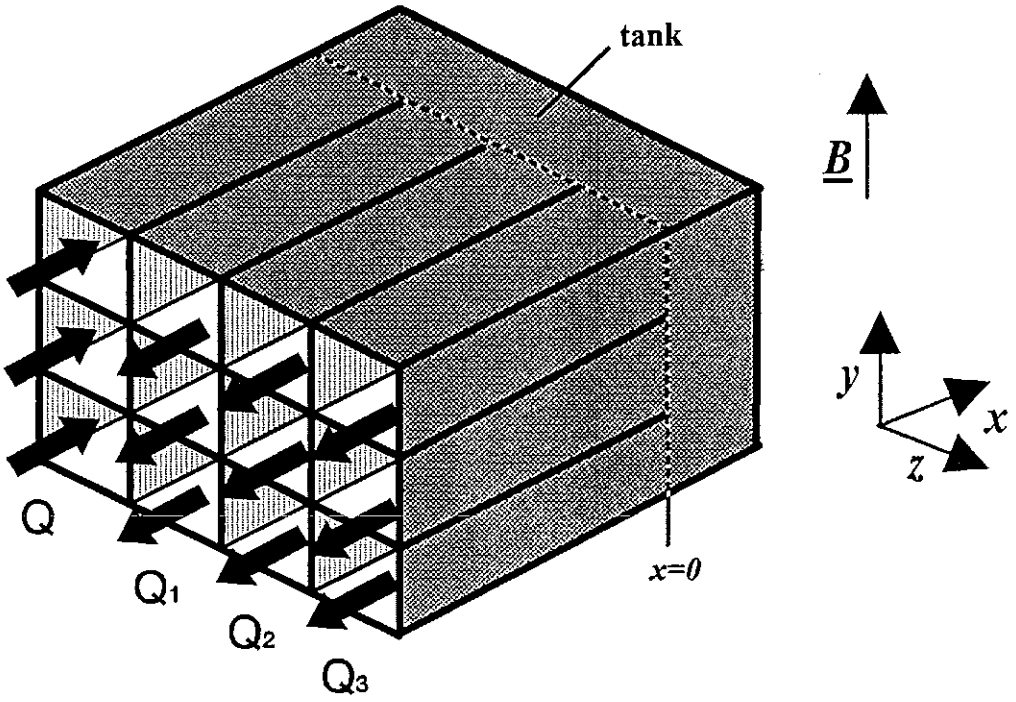

Fig. 17 Flow in a multi-layered 180°-turn. All straight channels have openings into a single tank.

6. Inertia effects

The solutions in the core presented in Sec. 5 are valid for $M>>1$ and $N>>1$, while viscous and inertia effects are confined to the side layers. The type of flow in the side layers depends on the relative magnitude of viscous, electromagnetic and inertia forces. Depending on the relation between N and M three different situations can be distinguished.

i) N>>M

The inertia terms in the side layer are negligible, while the flow in the layer is determined by **viscous-electromagnetic** interaction. This type of boundary layer has been considered in Sec. 4. The thickness of this layer is $O(M^{-\frac{1}{4}})$, while the 3-D pressure drop is

$$\Delta p_{3D} = O(M^{-1}). \qquad (14)$$

ii) N=O(M)

This type of layer is characterised by **viscous-electromagnetic-inertia** interaction. The thickness of the layer remains $O(M^{-\frac{1}{4}})$ or equivalently $O(N^{-\frac{1}{4}})$. All order-of-magnitude arguments used for $N>>M$ flow are valid for $N=O(M)$ flow. Since N is of the order M, the pressure drop is

$$\Delta p_{3D} = O(M^{-1}) = O\left((\alpha N)^{-1}\right) = O(N^{-1}). \qquad (15)$$

iii) N<<M

If $N<<M$, the side layer splits into two sublayers (Fig. 18). In the outer sublayer of thickness $O(N^{-\frac{1}{4}})$ there is **electromagnetic-inertia** balance of forces. The outer layer is thicker than inertialess layer *i)*. In the inner side layer of thickness $O(\mathrm{Re}^{-\frac{1}{4}})$ there is **viscous-inertia** interaction. This layer is thinner than inertialess side layer *i)*, and is in fact a usual, hydrodynamic, Prandtl layer. The interaction between the layers is based on the following mechanism. The outer layer conducts all electric current, which produces a longitudinal pressure gradient. This gradient passes unchanged into the inner layer and induces flow there. Since the pressure drop is created by the currents, the inner layer has no effect on the pressure drop (to the main order), and

$$\Delta p_{3D} = O(N^{-1}). \qquad (16)$$

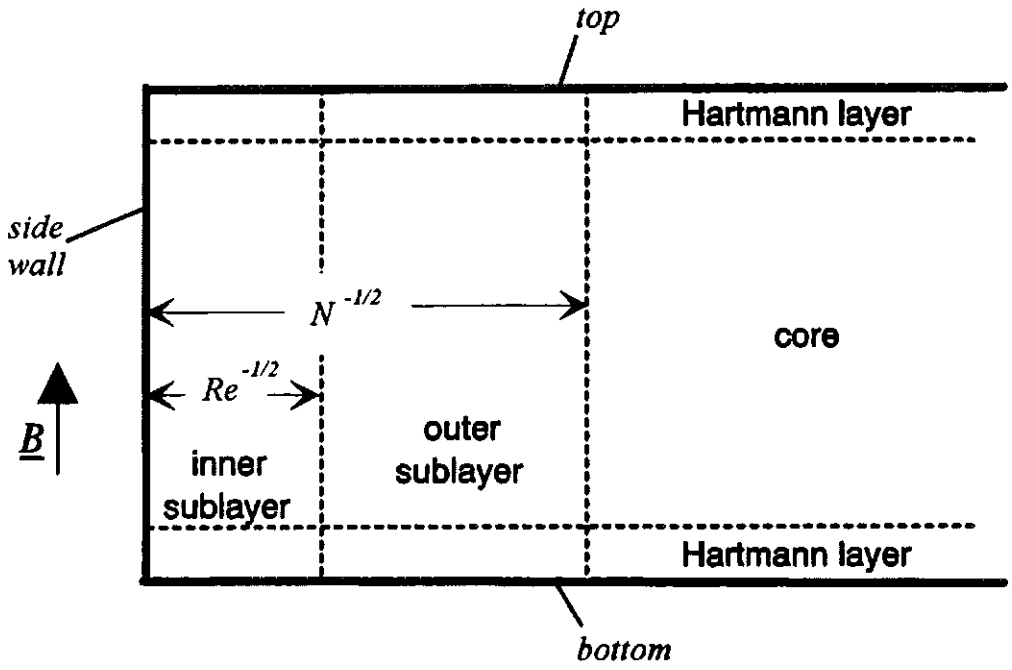

Fig. 18 Vicinity of the side wall and the structure of the side layer for $N<<M$.

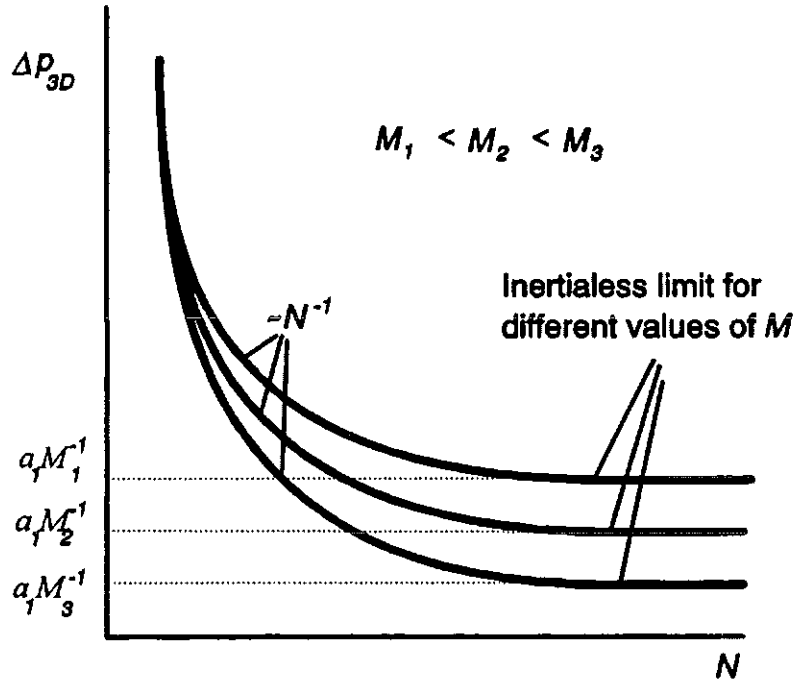

Fig. 19 Sketch of variation of the three-dimensional pressure drop with N.

Combining the results for all three cases one may construct the following expression for the 3-D pressure drop

$$\Delta p_{3D} = a_1 M^{-1} + a_2 N^{-1}. \qquad (17)$$

The constants $a_{1,2}$ depend on the duct geometry. Δp_{3D} is qualitatively sketched in Fig. 19 as a function of N and for different values of M. It should be noted that the decay of the pressure drop with increasing N is very fast. This can be compared to a much slower decay in ducts expanding in the direction of the field, where the following dependency is valid

$$\Delta p_{3D} = a_1 M^{-\frac{1}{2}} + a_2 N^{-\frac{1}{3}}. \qquad (18)$$

The expression (18) is based on the arguments of Tsinober & Stern (1964) and Hunt & Leibovich (1967) if applied to the side layers.

The result (17) is of fundamental importance for a self-cooled liquid-metal blanket design. It shows that if fluid velocity is small or if the magnetic field is very strong ($N>>M$) the 3-D pressure drop is of the order M^{-1}, the pressure drop in straight ducts per unit length. In moderate fields ($1<<N<<M$) it is of the same order (in the asymptotic sense) as the conventional, hydrodynamic pressure drop in ducts with no magnetic field. In fact, another normalisation for the pressure is to be used as that in hydraulics, namely $\frac{1}{2}\rho v_0^2$, instead of $\sigma a v_0 B_0^2$. This gives

$$\tfrac{1}{2}\Delta\bar{p}_{3D} = \frac{1}{2}\frac{\Delta p^*}{\frac{1}{2}\rho v_0^2} = N\Delta p_{3D} = a_2 + a_1\frac{N}{M} = a_2 + a_1\frac{M}{\mathrm{Re}} = a_2 + a_1\alpha^{-1}, \qquad (19)$$

where

$$\alpha = \frac{M}{N} = \frac{\mathrm{Re}}{M}$$

is a new parameter $O(1)$, p^* is a dimensional pressure and $\Delta\bar{p}_{3D}$ is a rescaled dimensionless 3-D pressure drop. Note that parameter α is "responsible" for instabilities and turbulence in MHD-flows (Branover, 1978, Moreau, 1990).

The discussion of inertia effects here is somewhat simplified since at low values of the interaction parameter separation effects at the edges and corners occur which may change the dependency (17). Nevertheless, in front and behind separation zones the present discussion still applies. There is an indication from the recent experiments in sharp elbows with manifolds and a T-junction that a large-scale separation zone is suppressed already at N~10 (Reimann, 1993). Separation itself may create vortices which would favour mixing of the coolant and thus improve heat transfer.

7. Conclusions

In poloidal channels of self-cooled liquid-metal blankets of rectangular cross-section a coolant flows with a constant velocity, so that the velocity profile is of slug type. The pressure drop per unit length is equal to M^{-1} in non-dimensional terms.

Order-of-magnitude estimates show that manifolds, expansions, contractions, elbows, etc. in the plane perpendicular to the magnetic field (poloidal-radial plane) cause additional pressure drop of the order of M^{-1}, i.e. the pressure drop in the straight duct per unit length, and thus may be neglected in the first approximation.

The asymptotic analysis performed for $M>>1$ and $N>>1$ demonstrates that viscous and inertia forces are confined to thin boundary layers, while the flow in the core is potential one. For $N>>M$ the side layers at the walls parallel to the magnetic field are of well-known parabolic inertialess nature, while for $N<<M$ a new type of the side layer has been obtained. It consists of two sublayers of thickness $O(N^{-1/2})$ (outer sublayer) and $O(\mathrm{Re}^{-1/2})$ (inner sublayer). For $N<<M$ the 3-D pressure drop is of the order of N^{-1}, i.e. the dimensional pressure drop is of the same order as the usual, hydrodynamic pressure drop. In fact, another scale for pressure is to be used, namely $\frac{1}{2}\rho v_0^2$ instead of $\sigma a v_0 B_0^2$. This is not to say that the magnetic field does not increase the pressure drop with respect to that in a hydrodynamic flow, but until N becomes of the order of M (in the asymptotic sense) the pressure drop is independent of B_0.

Flows in several basic geometries have been calculated. They demonstrate high reliability of poloidal concepts of liquid-metal blankets, since they guarantee uniform conditions for heat transfer. If changes of the duct cross-section occur in the plane perpendicular to the magnetic field (ideally the coolant should flow always in radial-poloidal plane) the disturbances are local and slug velocity profile is reached roughly at the distance equivalent to one duct width from the manifolds, expansions, etc.

Calculating flow patterns in flows in the plane perpendicular to the magnetic field is, in fact, a trivial matter in contrast to calculating the pressure drop required for pumping the liquid metal through the 3-D elements, since it requires numerical solution of the side layer equations (10) together with the boundary conditions. The side-layer problem will be treated in a subsequent investigation, especially for manifolds and expansions in the plane of the magnetic field for which the pressure drop is an important issue. For the flows considered here the pressure drop is not important.

Acknowledgement

This work has been performed in the framework of the Nuclear Fusion Project of the Kernforschungszentrum Karlsruhe and is supported by the European Communities within the European Fusion Technology Program.

8. References

Branover, H. *1978* Magnetohydrodynamic flow in ducts. *Jerusalem: Israel University Press.*

Bühler, L. & Molokov, S. *1993* Magnetohydrodynamic flows in ducts with insulating coatings. *Kernforschungszentrum Karlsruhe. Report KfK-5103.*

Hunt, J.C.R. & Leibovich, S. *1967* Magnetohydrodynamic flows in channels of variable cross-section with strong transverse magnetic field. *J. Fluid Mech.* **28**, 241-260.

Hunt, J.C.R. & Ludford, G.S.S. *1968* Three-dimensional MHD duct flows with strong transverse magnetic fields. Part 1. Obstacles in a constant-area channel. *J. Fluid Mech.* **33**, 693-714.

Kulikovskii, A.G. *1968* Slow steady flows of a conducting fluid at large Hartmann numbers. *Fluid Dynamics.* **3** (2), 1-5.

Lavrentiev, I.V., Molokov, S.Yu., Sidorenkov, S.I. & Shishko, A.Ya. *1990* Stokes flow in a rectangular magnetohydrodynamic channel with nonconducting walls within a nonuniform magnetic field at large Hartmann numbers, Magnetohydrodynamics, **26** (3), 328-338.

Malang, S., Bojarsky, E., Bühler, L., Deckers, H., Fischer, U., Norajitra, P. & Reiser, H. *1993* Dual coolant liquid metal breeder concept. *Proc. 17th Symposium on Fusion Technology, Rome, Italy, 14-18 September 1992,* vol. **2**, 1424-1428.

Molokov, S. *1990* Magnetohydrodynamic flow in a rectangular channel in a strong skewed magnetic field. *Proc. 13th Riga Conference on Magnetohydrodynamics,* Riga 1990, Pt. 1, pp. 23-24 (In Russian).

Molokov, S. & Bühler, L. *1993* Numerical simulation of liquid-metal flows in radial-toroidal-radial bends. *Kernforschungszentrum Karlsruhe. Report KfK 5160.*

Molokov, S. & Bühler, L. *1994* Liquid metal flow in a U-bend in a strong uniform magnetic field. *J.Fluid Mech.* (to be published)

Molokov, S. & Shishko, A. *1993* Fully developed magnetohydrodynamic flows in rectangular ducts with insulating walls. *Kernforschungszentrum Karlsruhe. Report KfK 5247.*

Moreau, R. *1990* Magnetohydrodynamics. *Dordrecht-Boston-London: Kluwer.*

Reed, C.B. & Picologlou, B.F. *1989* Sidewall flow instabilities in liquid metal MHD flow under blanket relevant conditions. *Fusion Technology.* **15,** 705-715.

Reimann, J. *1993* Private communication.

Roberts, P.H. *1967* An introduction to magnetohydrodynamics. *Longmans.*

Shercliff, J.A. *1953* Steady motion of conducting fluids in pipes under transverse magnetic fields. *Proc. Cambr. Philos. Soc.* **49**, pp. 136-144.

Sze, D.K., Mattas, R.F., Hull, A.B., Picologlou, B. & Smith, D.L. *1992* MHD considerations for a self-cooled liquid lithium blanket. *Fusion Technology.* **21** (3), Pt 2b, 2099-2106.

Temperley D.J. *1976* Magnetohydrodynamic flow in a rectangular duct under a uniform transverse magnetic field at high Hartmann number. *Archives of Mechanics.* **28** (5-6), 947-968.

Tsinober, A. & Stern, A. *1964* A similar stagnation-point magnetohydrodynamic flow. *Izvestija Akademii Nauk Latv. SSR, Ser. fiziko-tehnicheskih nauk.* No. 1, 15-19 (In Russian).

Vatazhin, A.B., Liubimov, G.A. & Regirer, S.A. *1970* Magnetohydrodynamic channel flows. *Moscow: Nauka* (In Russian).

Walker, J.S., Ludford, G.S.S. & Hunt, J.C.R. *1972* Three-dimensional MHD duct flows with strong transverse magnetic fields. Part 3. Variable-area rectangular ducts with insulating walls. *J. Fluid Mech.* **56**, 121-141.